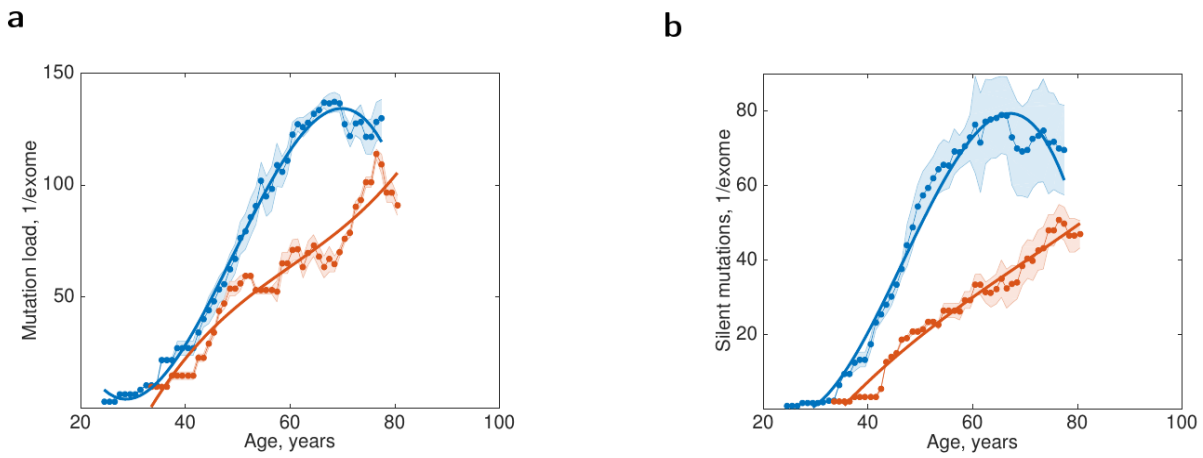

Supplementary Figure 1 | Characteristic somatic mutation load in bladder urothelial carcinoma (BLCA). Men (blue) vs. women (red). **a.** BI, IlluminaGA DNASeq, automated pipeline, all mutations. **b.** BI, IlluminaGA, DNASeq, automated pipeline, silent mutations only.

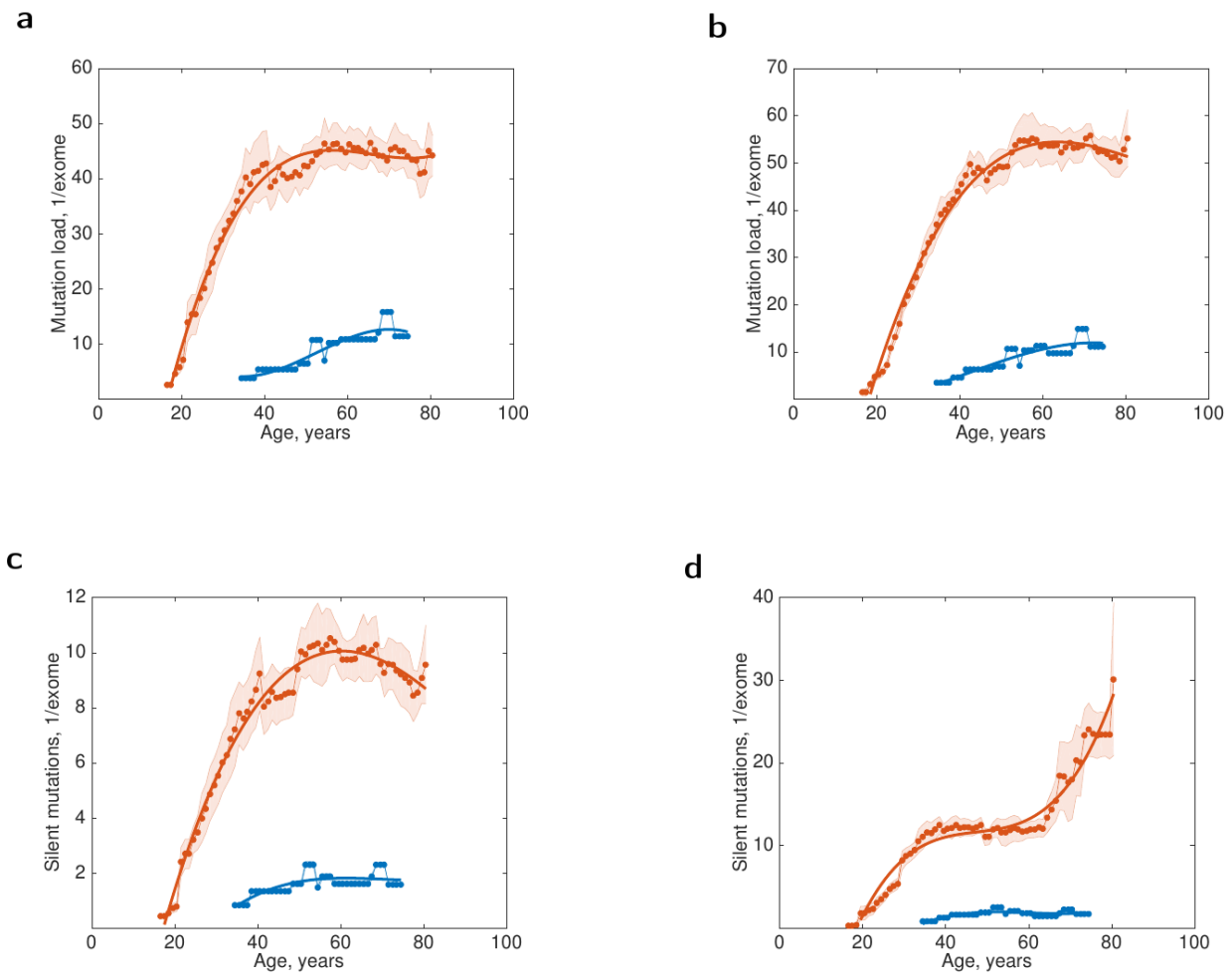

Supplementary Figure 2 | Characteristic somatic mutation load in breast invasive carcinoma (BRCA). Men (blue) vs. women (red). a. WUSM, IlluminaGA DNASeq, automated pipeline, all mutations. **b**. WUSM, IlluminaGA, DNASeq, curated pipeline, all mutations. **c.** WUSM, IlluminaGA DNASeq, silent mutations only. **d.** WUSM, IlluminaGA DNASeq, curated pipeline, silent mutations only.

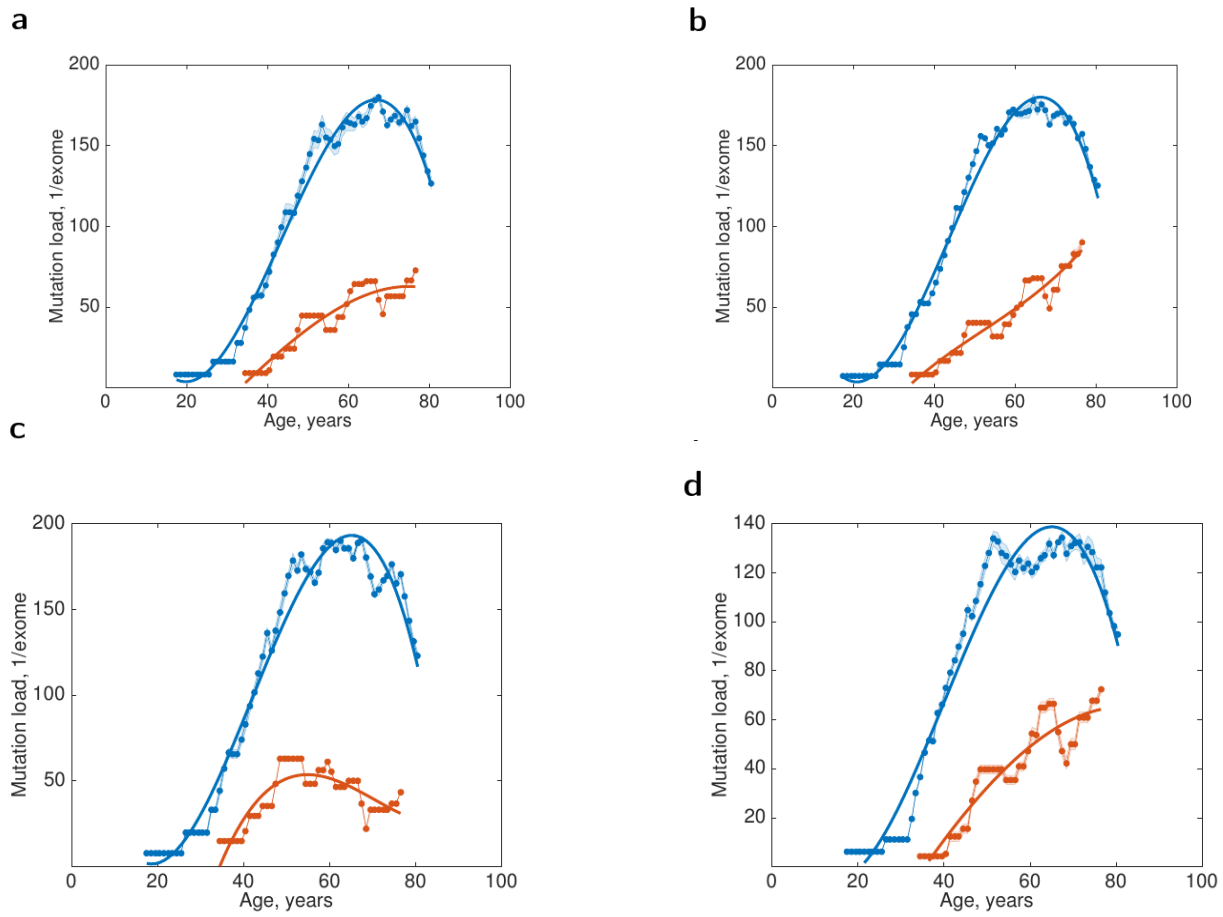

Supplementary Figure 3 | Characteristic somatic mutation load in esophageal carcinoma (ESCA), all mutations. Men (blue) vs. women (red). **a**. BCGSC, IlluminaHISeq DNASeq, automated pipeline. **b**. BI, IlluminaGA, automated pipeline. **c.** BCM, IlluminaGA DNASeq, automated pipeline. **d.** UCSC, IlluminaGA, IlluminaGA DNASeq, automated pipeline.

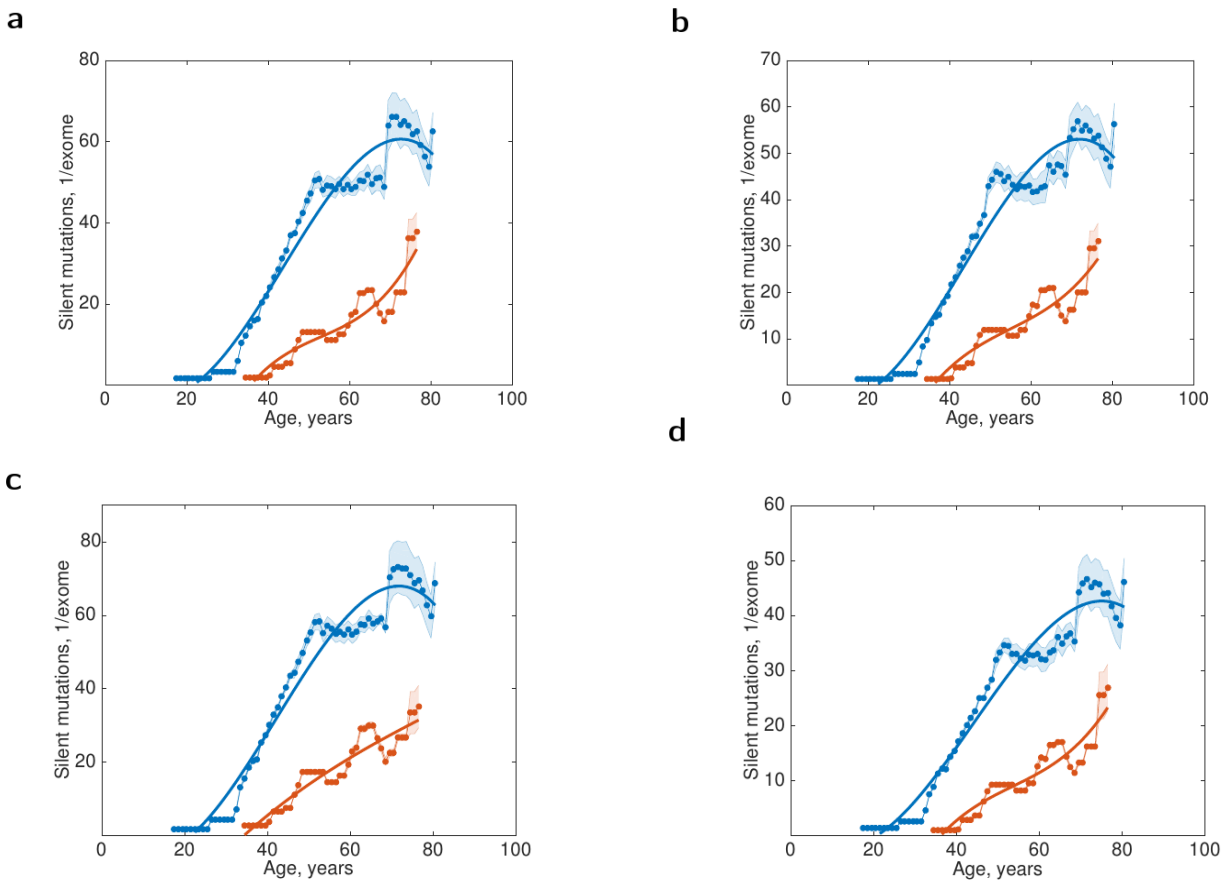

Supplementary Figure 4 | Characteristic somatic mutation load in esophageal carcinoma (ESCA), silent mutations only. Men (blue) vs. women (red). **a.** BSGSC, IlluminaHiSeq DNASeq, automated pipeline. **b.** BI, IlluminaGA, automated pipeline. **c.** BCM, IlluminaGA DNASeq, automated pipeline. **d.** UCSC, IlluminaGA, automated pipeline.

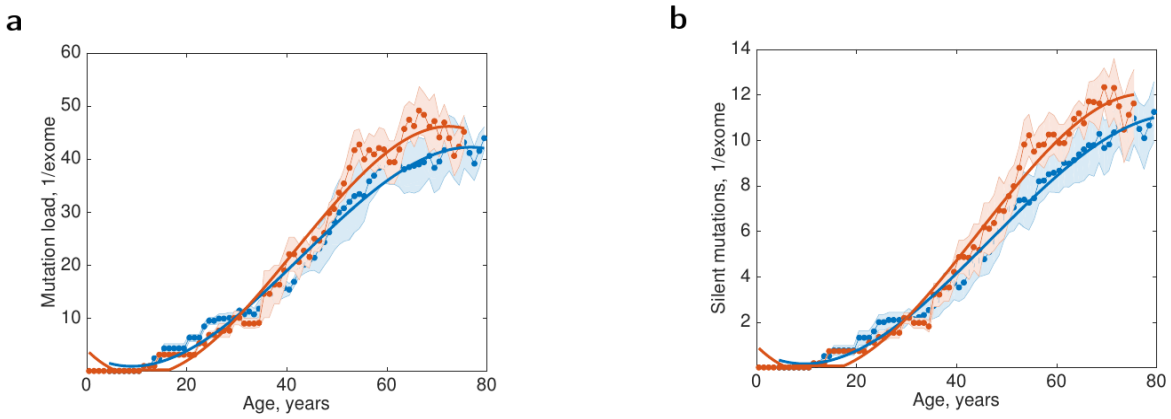

Supplementary Figure 5 | Characteristic somatic mutation load in glioblastoma multiforme (GBM). Men (blue) vs. women (red). **a.** BI, IlluminaGA DNASeq, all mutations. **b.** BI, IlluminaGA DNASeq, silent mutations only.

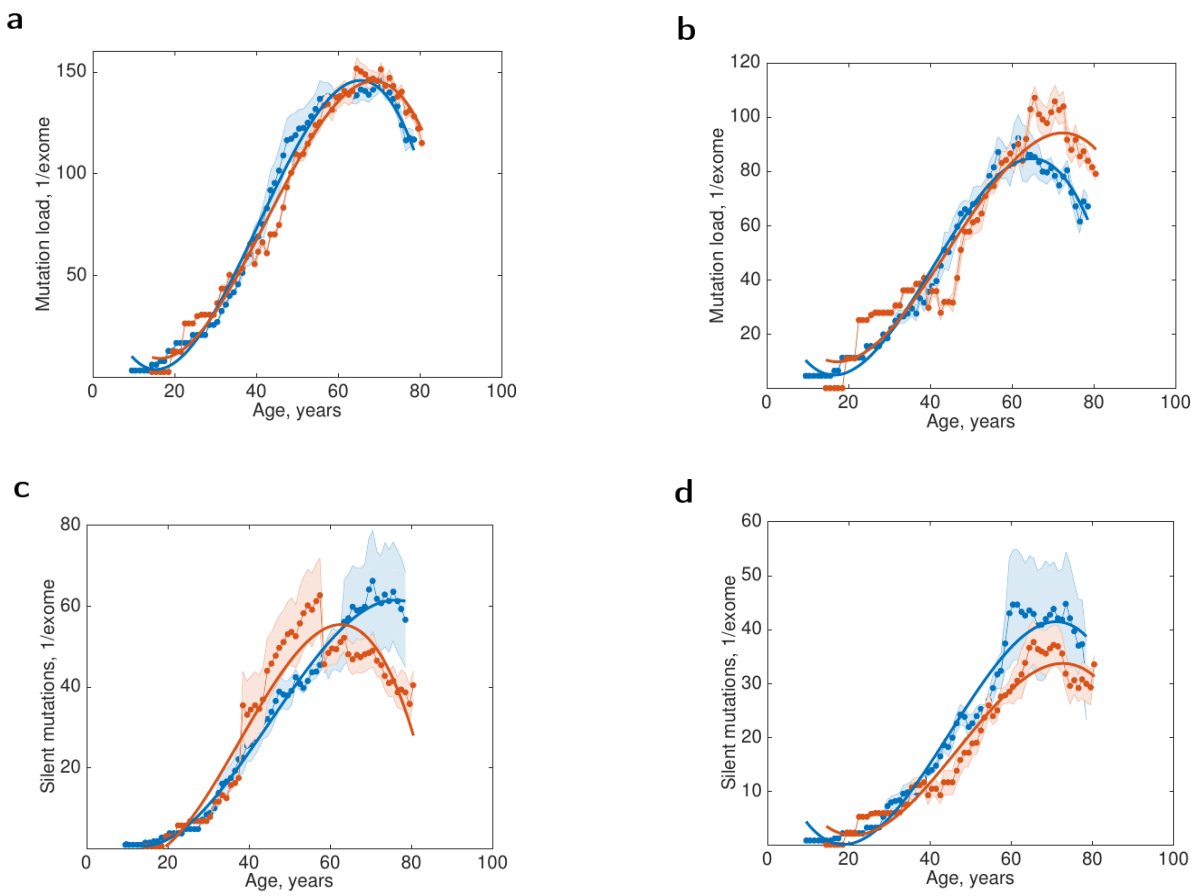

Supplementary Figure 6 | Characteristic somatic mutation load in head and neck squamous cell carcinoma (HNSC). Men (blue) vs. women (red). **a.** BI, IlluminaGA DNASeq, automated pipeline, all mutations. **b.** BI, IlluminaGA DNASeq, all mutations. **c.** BI, IlluminaGA DNASeq, automated pipeline, silent mutations only. **d.** BI, IlluminaGA DNASeq, silent mutations only.

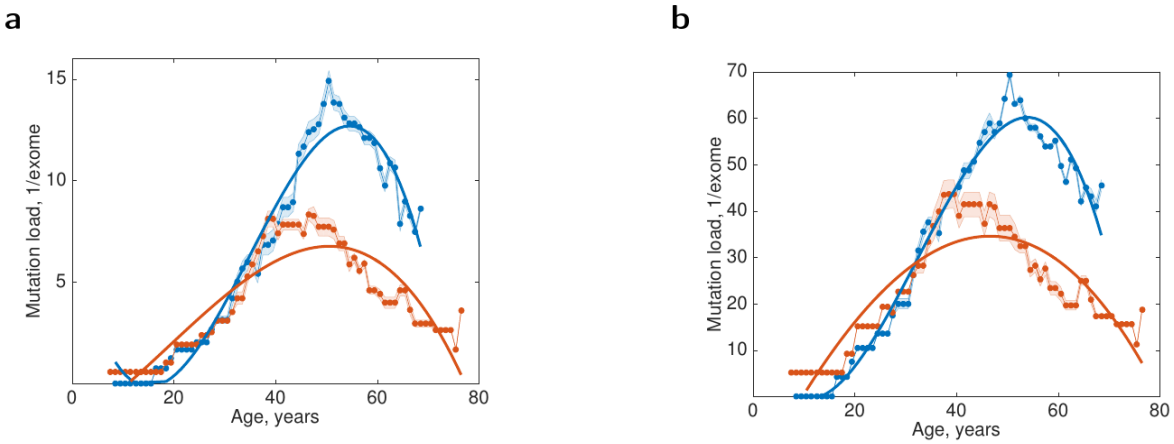

Supplementary Figure 7 | Characteristic somatic mutation load in kidney chromophobe (KICH), all mutations. Men (blue) vs. women (red). **a.** BCM, IlluminaGA DNASeq. **b.** BCM, mixed IlluminaGA DNASeq and SOLiD.

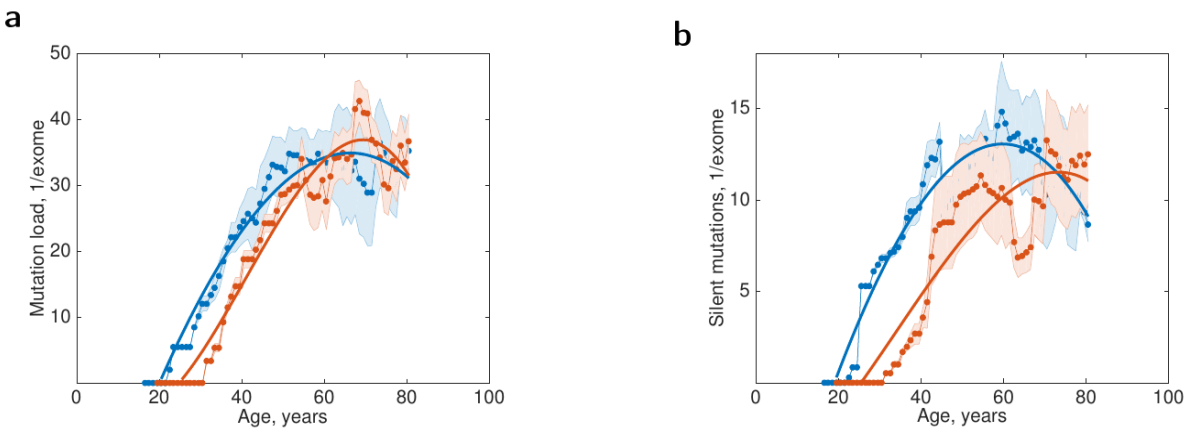

Supplementary Figure 8 | Characteristic somatic mutation load in kidney renal clear cell carcinoma (KIRC). Men (blue) vs. women (red). **a.** BI, IlluminaGA DNASeq, automated pipeline, all mutations. **b.** BCM, mixed IlluminaGA and SOLiD, silent mutations only.

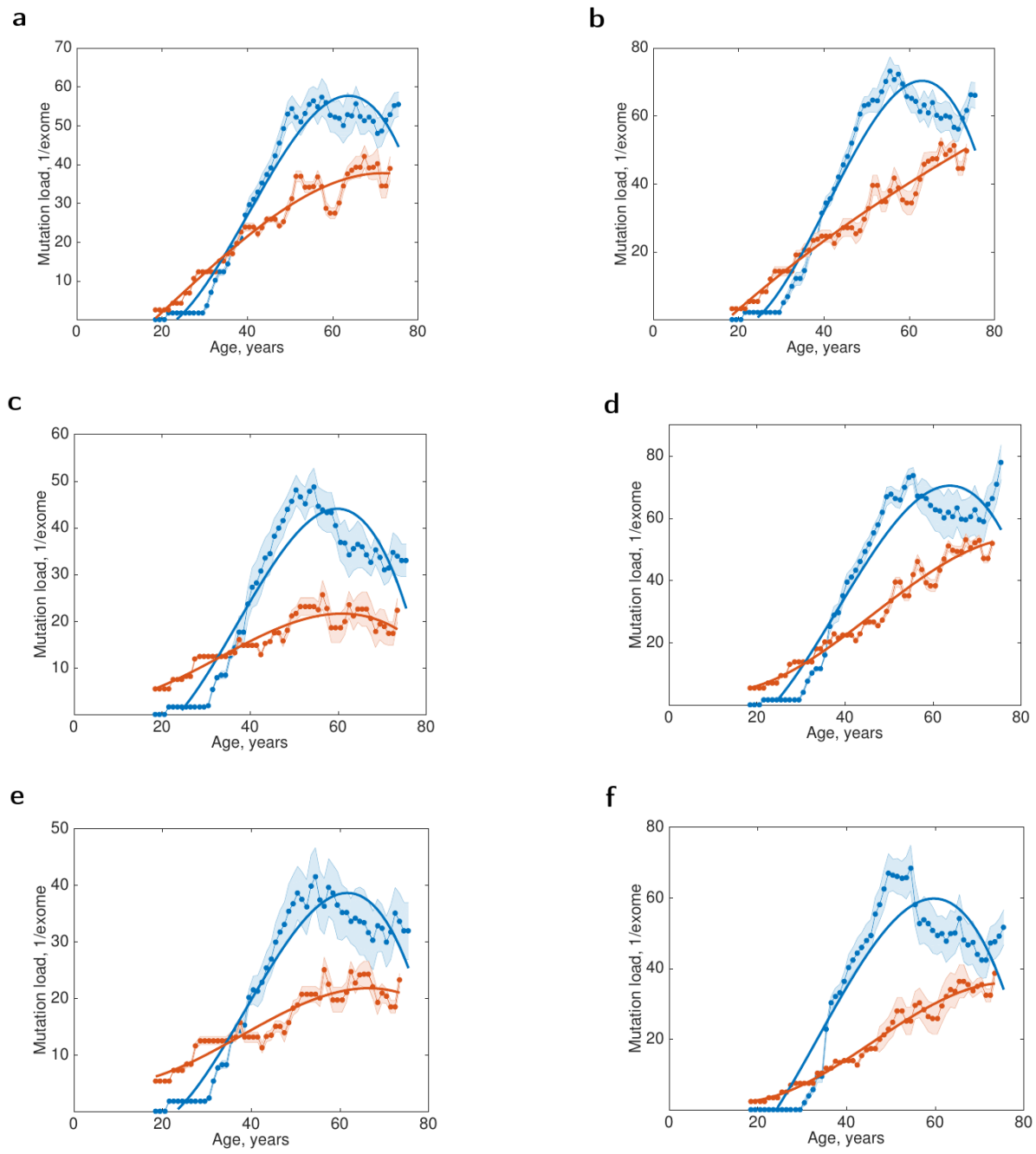

Supplementary Figure 9 | Characteristic somatic mutation load in kidney renal papillary cell carcinoma (KIRP), all mutations. Men (blue) vs. women (red). **a.** BCM, IlluminaGA DNASeq, curated pipeline. **b.** BCM, mixed IlluminaGA and SOLiD. **c.** BI, IlluminaGA DNASeq, automated pipeline. **d.** BI, IlluminaGA DNASeq, curated pipeline. **e.** BI, IlluminaGA DNASeq. **f.** UCSC, IlluminaGA DNASeq, automated pipeline.

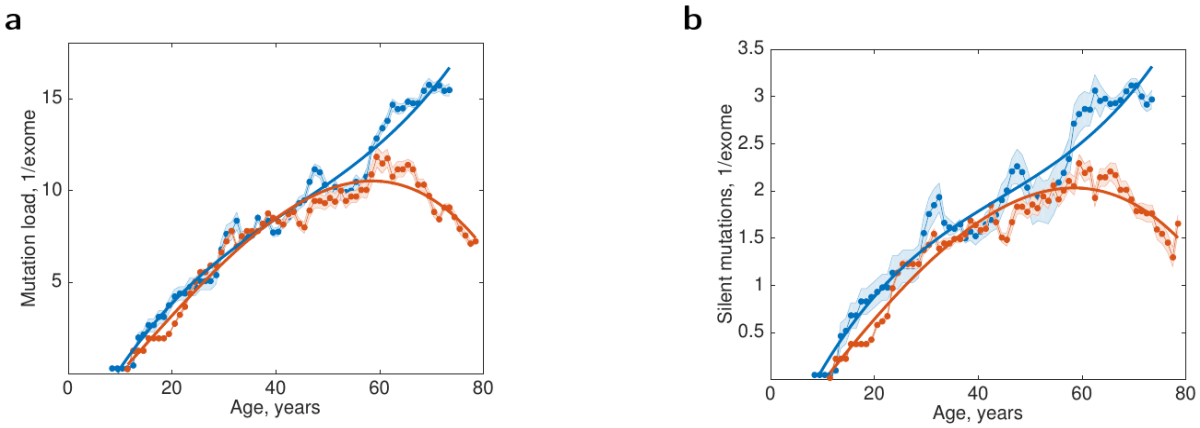

Supplementary Figure 10 | Characteristic somatic mutation load in acute myeloid leukemia (LAML). Men (blue) vs. women (red). **a.** WUSM, IlluminaGA DNASeq, all mutations. **b.** WUSM, IlluminaGA DNASeq, silent mutations only.

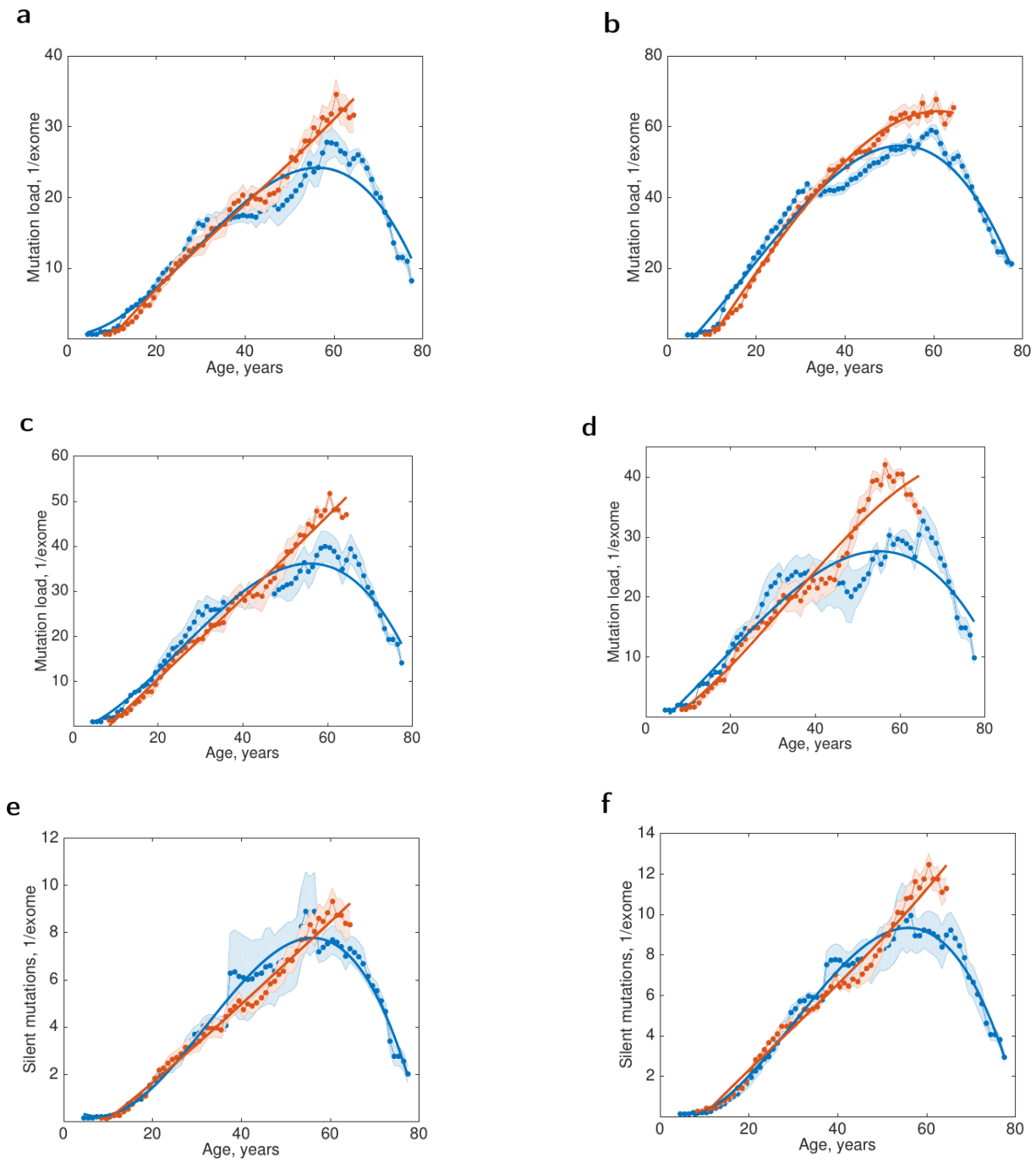

Supplementary Figure 11 | Characteristic somatic mutation load in brain lower grade glioma (LGG). Men (blue) vs. women (red). **a.** BCM, IlluminaGA DNASeq, automated pipeline, all mutations. **b.** BI, IlluminaGA DNASeq, curated pipeline, all mutations. **c.** BI, IlluminaGA DNASeq, all mutations. **d.** BI, IlluminaGA DNASeq, curated pipeline, silent mutations only. **e.** BCM, IlluminaGA DNASeq, automated pipeline, silent mutations only. **f.** BI, IlluminaGA DNASeq, silent mutations only.

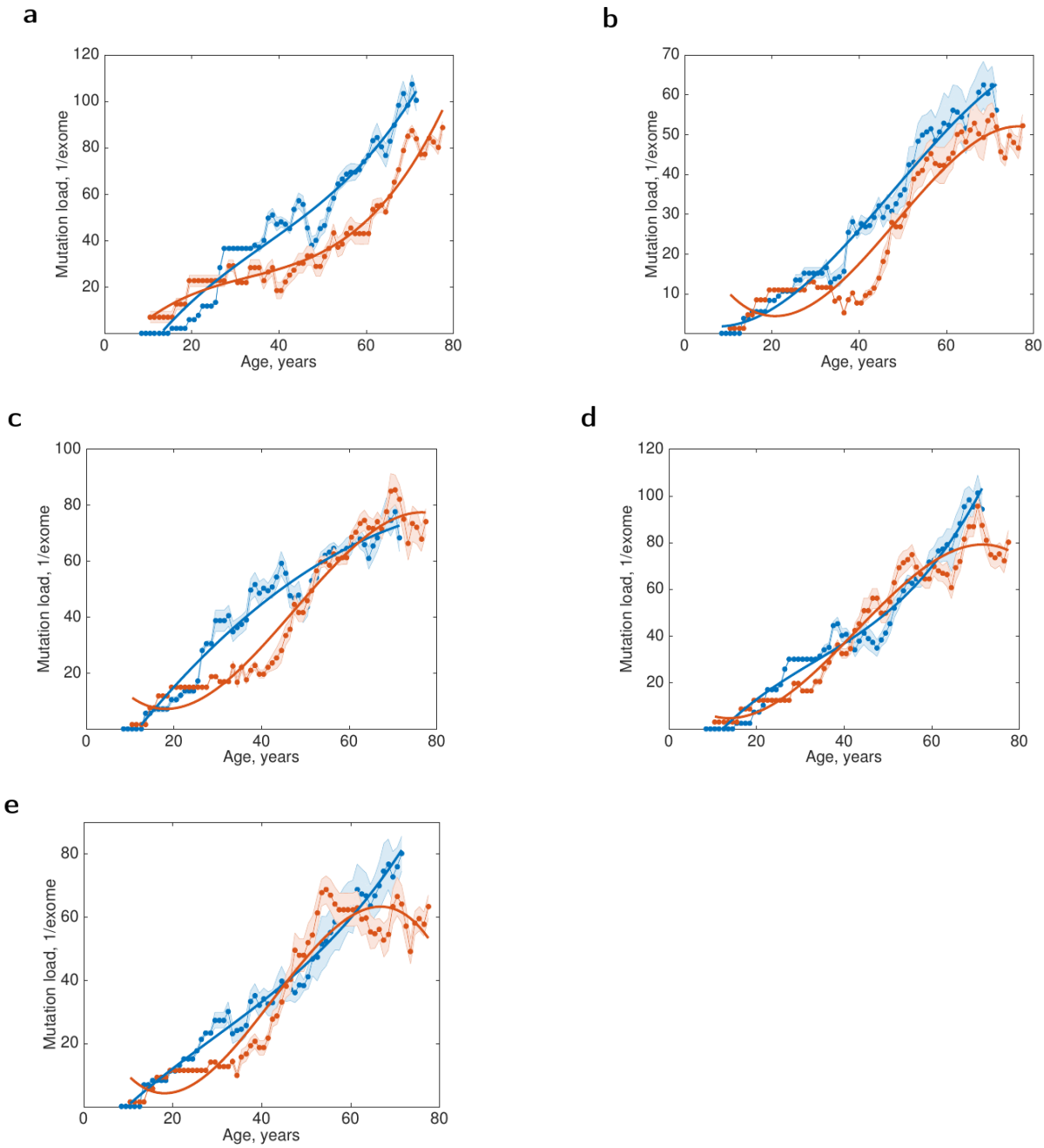

Supplementary Figure 12 | Characteristic somatic mutation load in liver hepatocellular carcinoma (LIHC), all mutations. Men (blue) vs. women (red). **a.** BCGSC, IlluminaHiSeq DNASeq, automated pipeline. **b.** BCM, IlluminaGA DNASeq, automated pipeline. **c.** BCM, mixed IlluminaGA and SOLiD, curated pipeline. **d.** BI, IlluminaGA DNASeq, automated pipeline. **e.** UCSC, IlluminaGA DNASeq, automated pipeline.

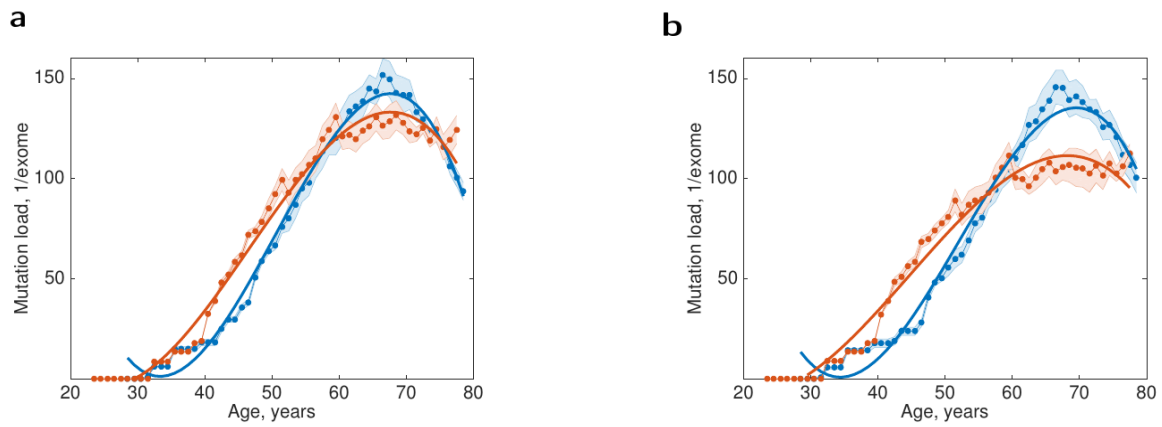

Supplementary Figure 13 | Characteristic somatic mutation load in lung adenocarcinoma (LUAD). Men (blue) vs. women (red). **a.** BI, IlluminaGA DNASeq, automated pipeline, all mutations. **b.** BI, IlluminaGA DNASeq, all mutations.

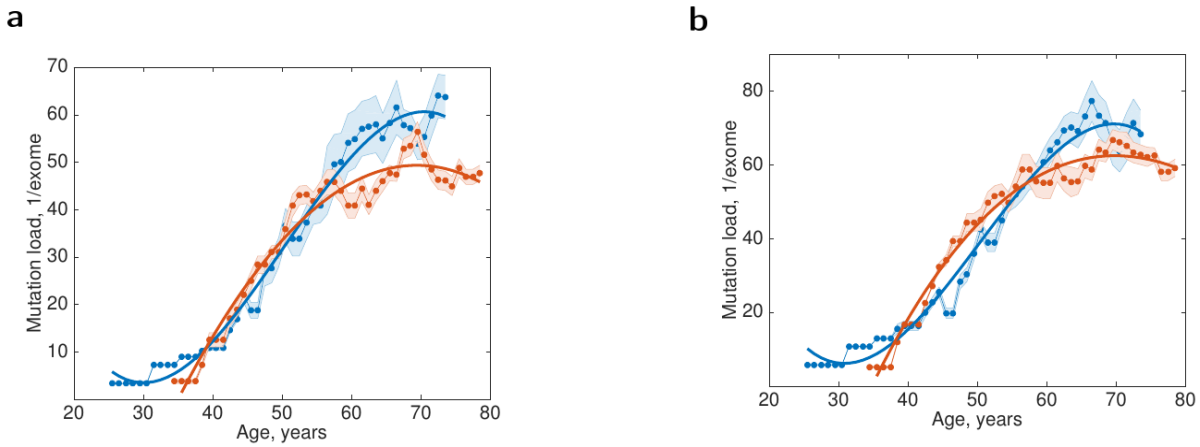

Supplementary Figure 14 | Characteristic somatic mutation load in pancreatic adenocarcinoma (PAAD), all mutations. Men (blue) vs. women (red). **a.** BCGSC, IlluminaHiSeq DNASeq, automated pipeline. **b.** BI, IlluminaGA DNASeq, automated pipeline.

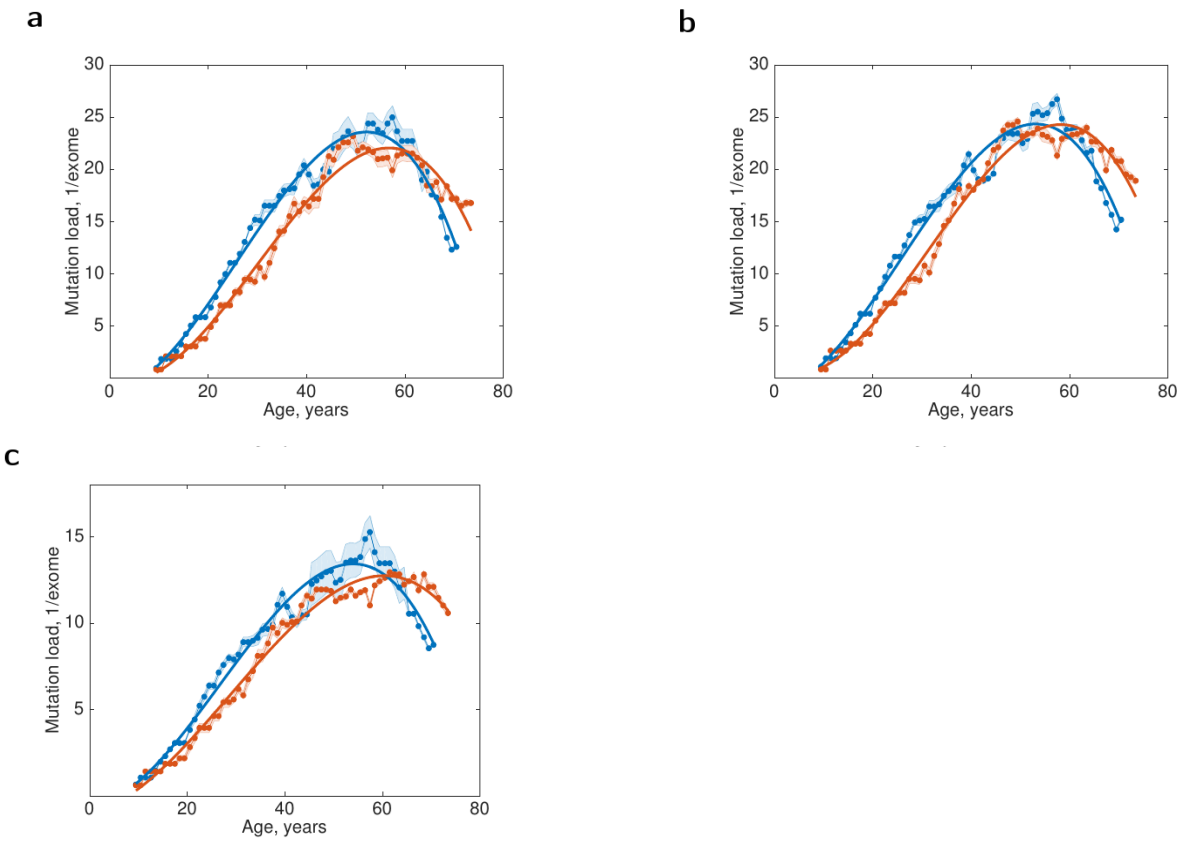

Supplementary Figure 15 | Characteristic somatic mutation load in pheochromocytoma and paraganglioma (PCPG), all mutations. Men (blue) vs. women (red). **a.** BCM, IlluminaGA DNASeq, automated pipeline. **b.** BI, IlluminaGA DNASeq, automated pipeline. **c.** UCSC, IlluminaGA DNASeq, automated pipeline.

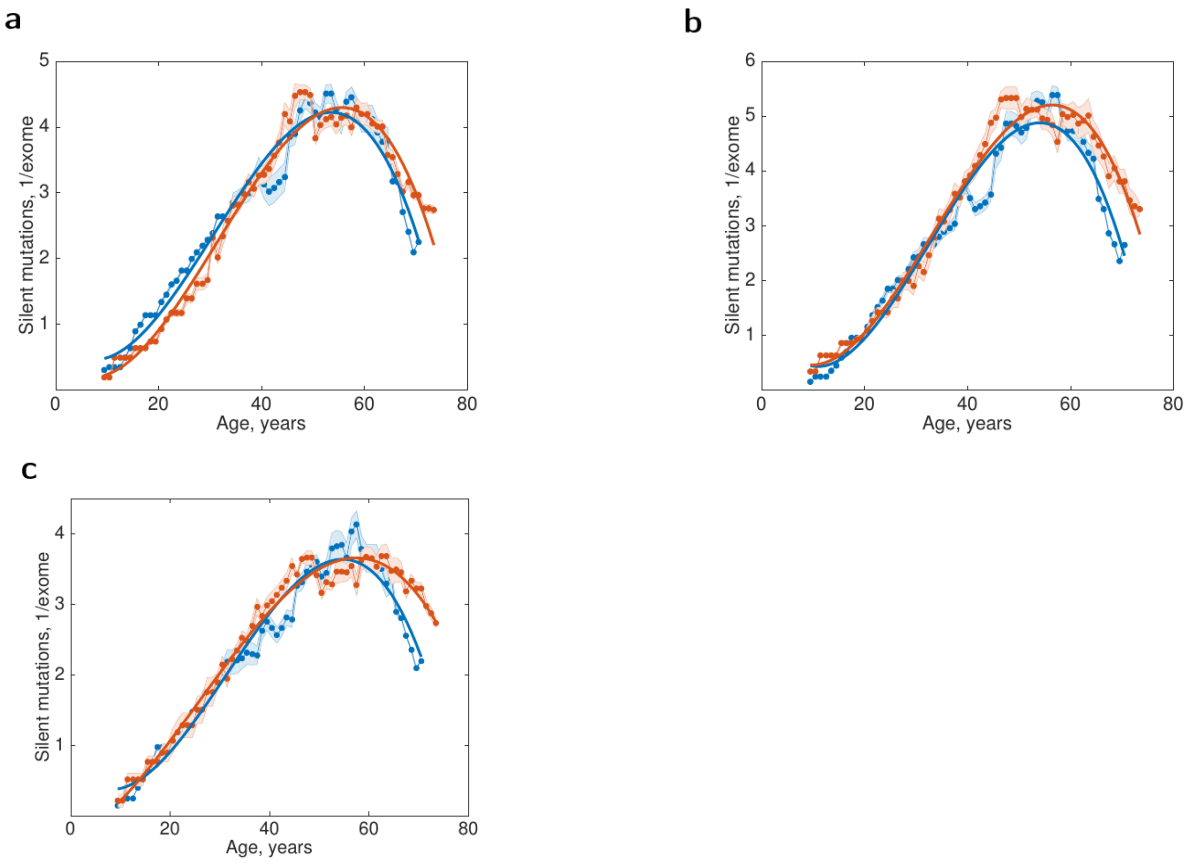

Supplementary Figure 16 | Characteristic somatic mutation load in pheochromocytoma and paraganglioma (PCPG), silent mutations only. Men (blue) vs. women (red). **a.** BCM, IlluminaGA DNASeq, automated pipeline. **b.** BI, IlluminaGA DNASeq, automated pipeline. **c.** UCSC, IlluminaGA DNASeq, automated pipeline.

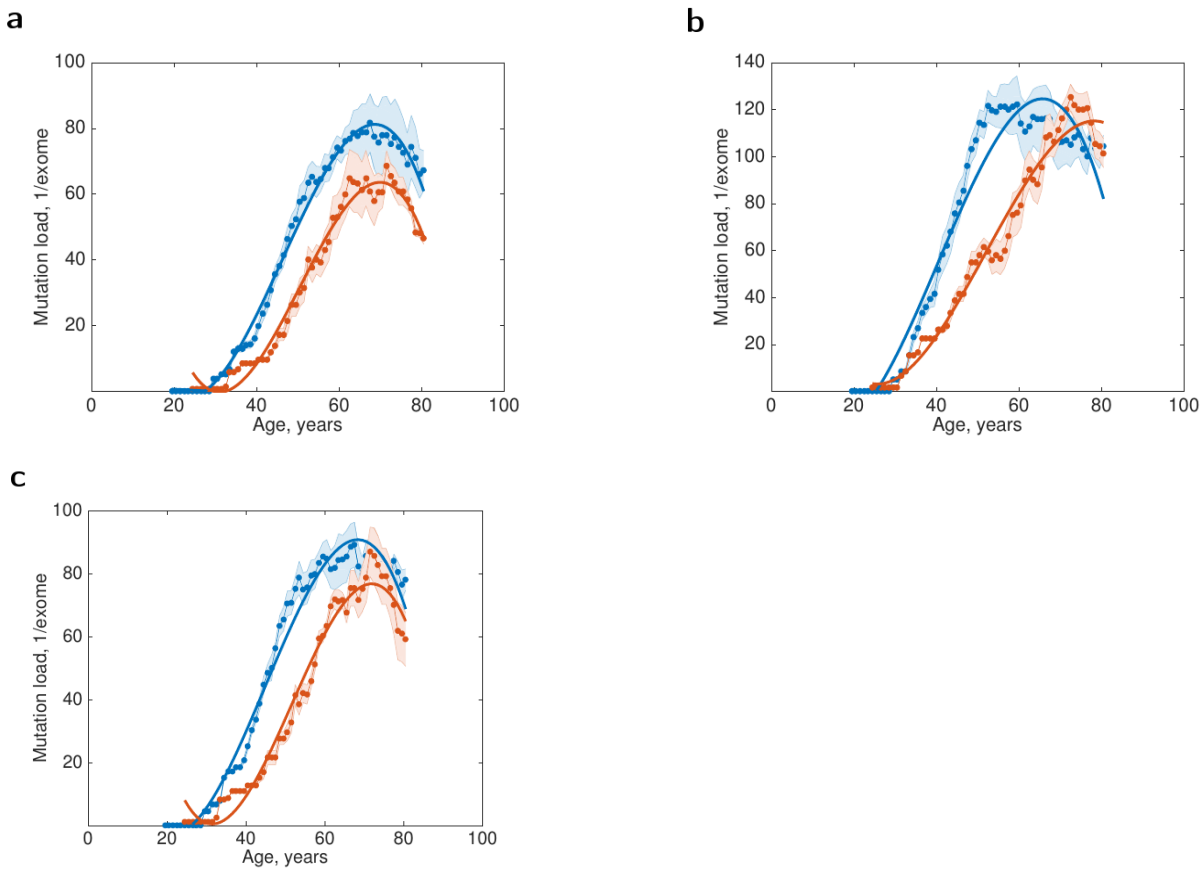

Supplementary Figure 17 | Characteristic somatic mutation load in stomach adenocarcinoma (STAD), all mutations. Men (blue) vs. women (red). **a.** BCM, IlluminaGA DNASeq, automated pipeline. **b.** BI, IlluminaGA DNASeq, automated pipeline. **c.** BI, IlluminaGA DNASeq, curated pipeline.

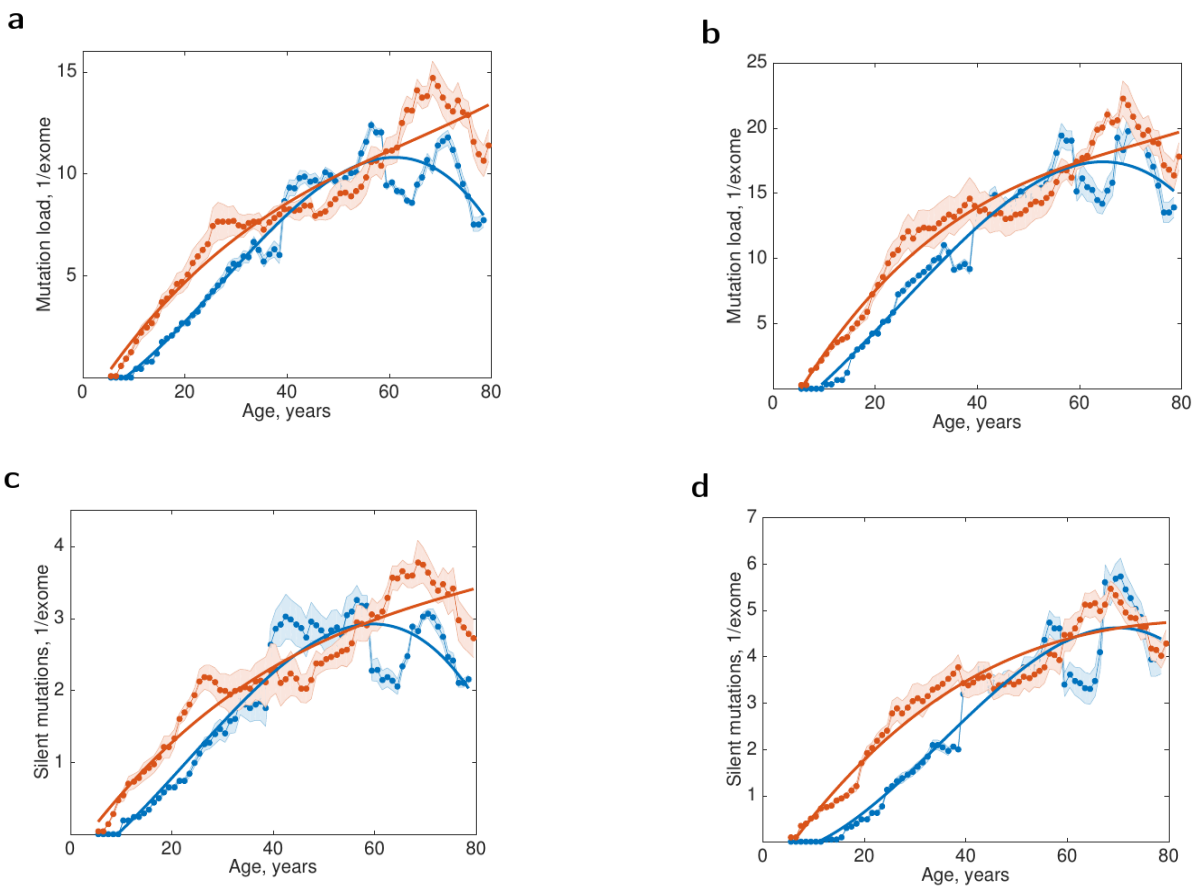

Supplementary Figure 18 | Characteristic somatic mutation load in thyroid carcinoma (THCA). Men (blue) vs. women (red). **a.** BCM, IlluminaGA DNASeq, automated pipeline, all mutations. **b.** BI, IlluminaGA DNASeq, all mutations. **c.** BCM, IlluminaGA DNASeq, automated pipeline, silent mutations only. **d.** BI, IlluminaGA DNASeq, silent mutations only.

Characteristic somatic mutation load vs. cancer incidence

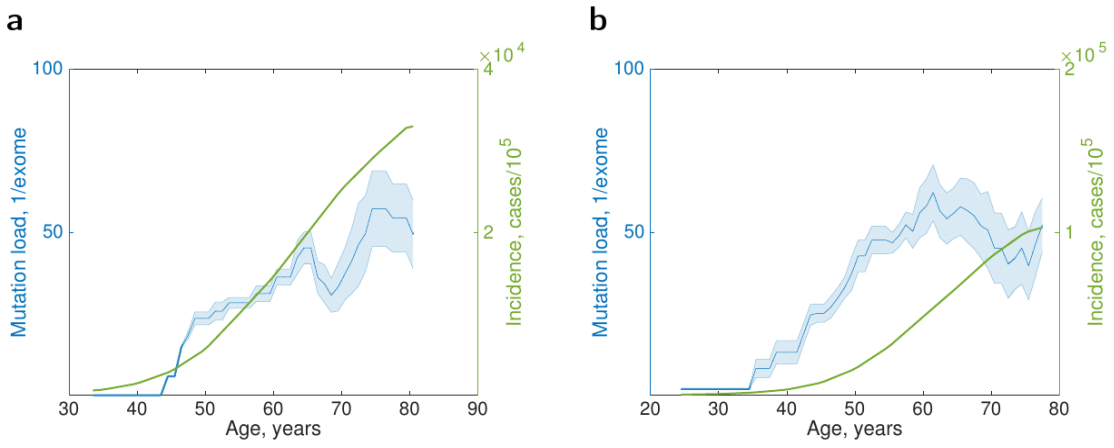

Supplementary Figure 19 | Characteristic somatic mutation load vs. cancer incidence in bladder urothelial carcinoma (BLCA). **a.** Women, BI, IlluminaGA DNASeq, curated pipeline. **b.** Men, BI, IlluminaGA DNASeq, curated pipeline.

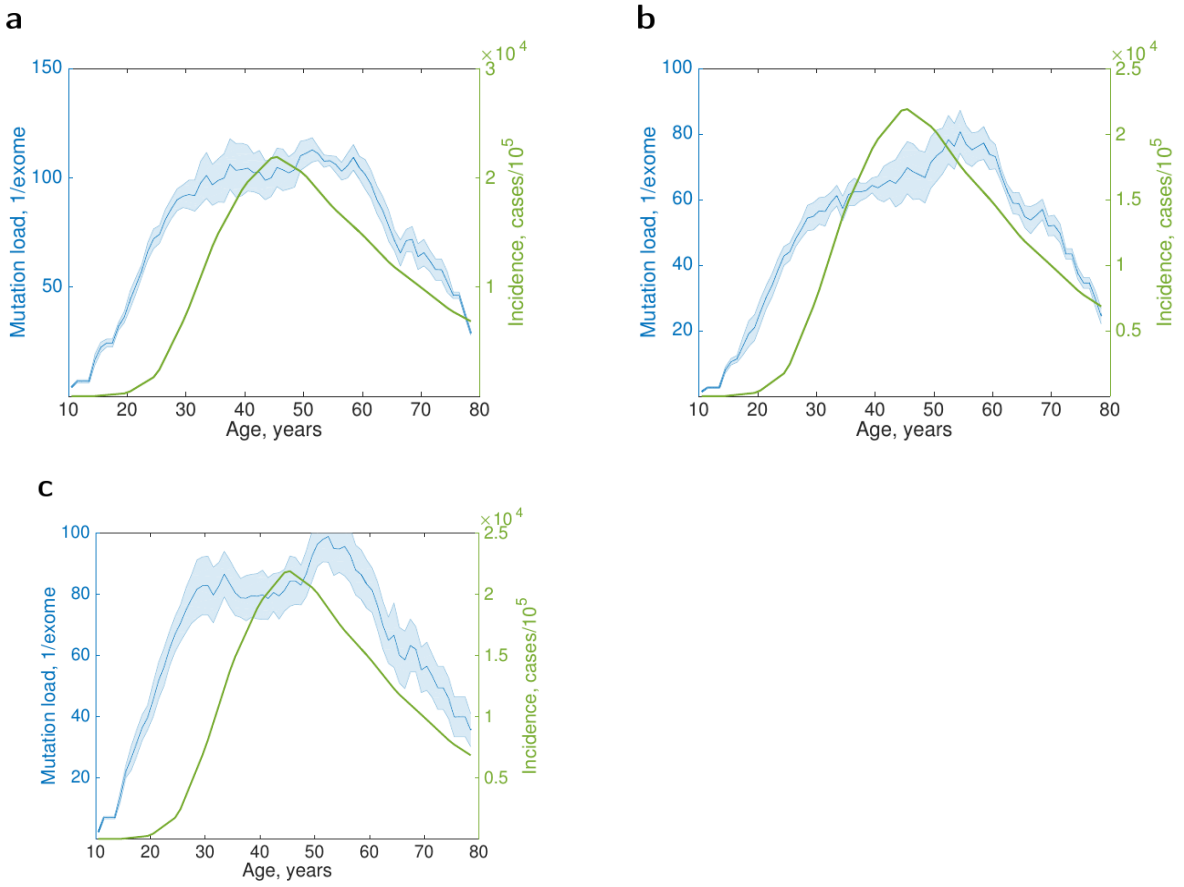

Supplementary Figure 20 | Characteristic somatic mutation load vs. cancer incidence in cervical squamous cell carcinoma and endocervical adenocarcinoma (CESC). **a.** BCGSC, IlluminaHiSeq, automated pipeline. **b.** UCSC, IlluminaGA, automated pipeline. **c.** WUSM, IlluminaGA, curated pipeline.

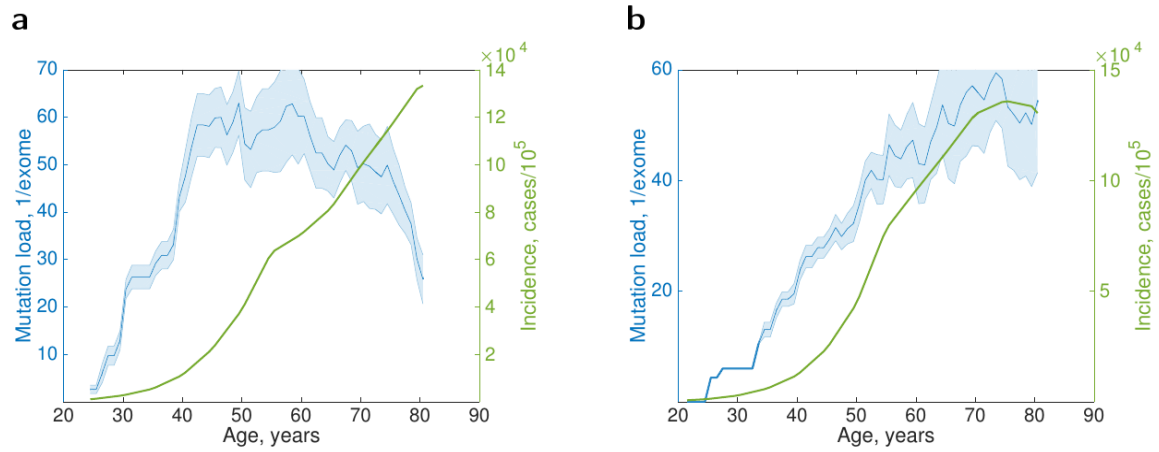

Supplementary Figure 21 | Characteristic somatic mutation load vs. cancer incidence in colon adenocarcinoma (COAD). **a.** Women, BCM, IlluminaGA. **b.** Men, BCM, IlluminaGA.

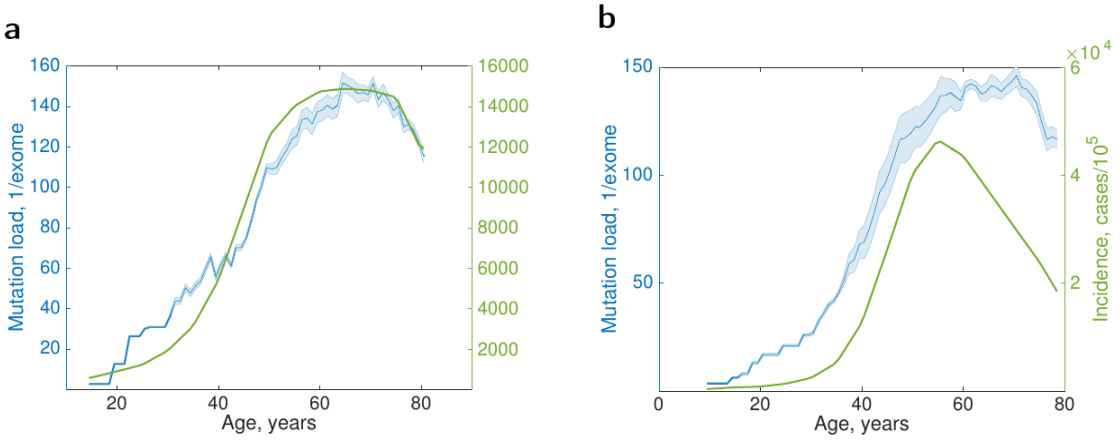

Supplementary Figure 22 | Characteristic somatic mutation load vs. cancer incidence in head and neck squamous cell carcinoma (HNSC). **a.** Women, BI, IlluminaGA, automated pipeline. **b.** Men, BI, IlluminaGA, automated pipeline.

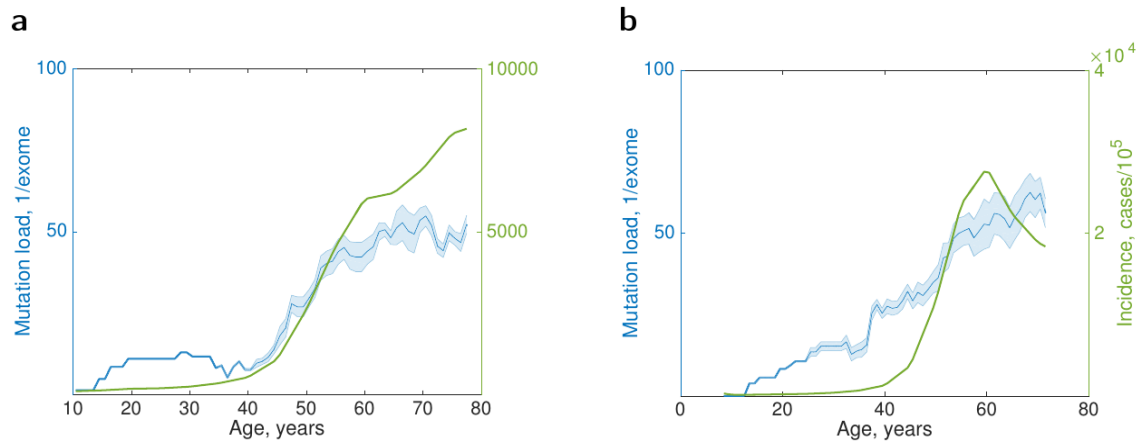

Supplementary Figure 23 | Characteristic somatic mutation load vs. cancer incidence in liver hepatocellular carcinoma (LIHC). **a.** Women, BCM, IlluminaGA, automated pipeline. **b.** Men, BCM, IlluminaGA, automated pipeline.

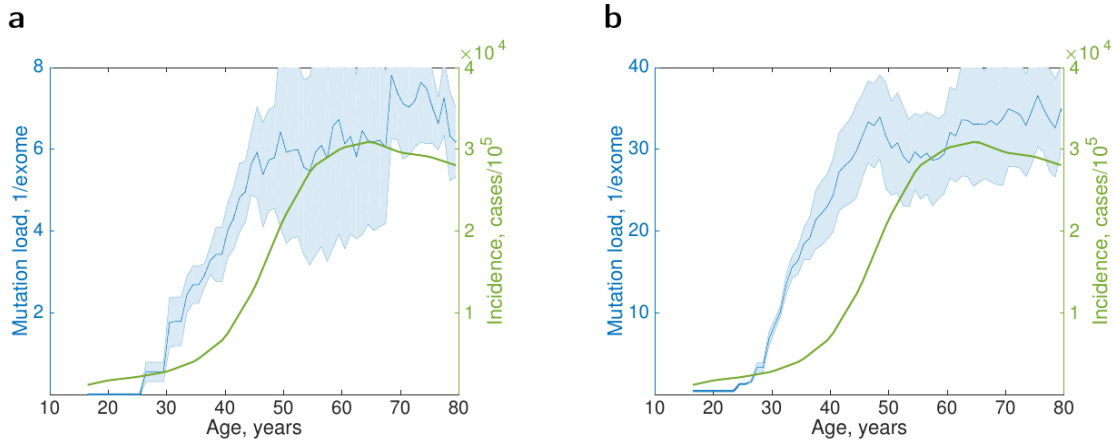

Supplementary Figure 24 | Characteristic somatic mutation load vs. cancer incidence in ovarian serous cystadenocarcinoma (OV). **a.** BCM, SOLiD, curated pipeline. **b.** WUSM, IlluminaGA.

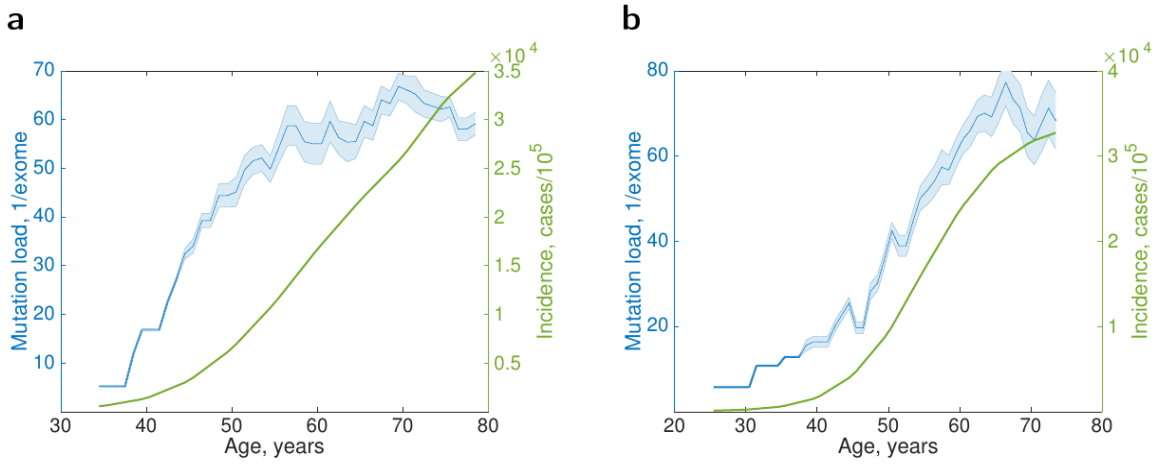

Supplementary Figure 25 | Characteristic somatic mutation load vs. cancer incidence in pancreatic adenocarcinoma (PAAD). **a.** Women, BCM, IlluminaGA, automated pipeline. **b.** Men, BCM, IlluminaGA, automated pipeline.

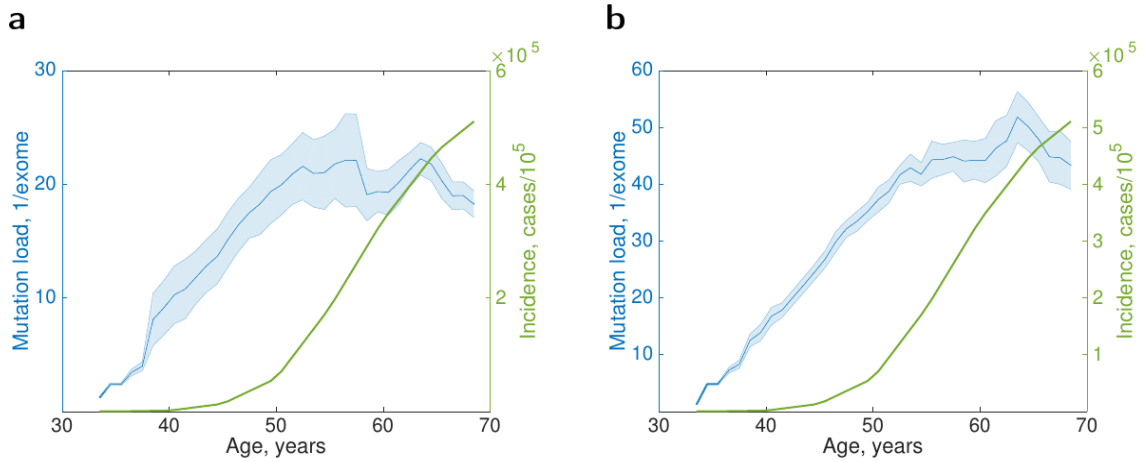

Supplementary Figure 26 | Characteristic somatic mutation load vs. cancer incidence in prostate adenocarcinoma (PRAD). **a.** BCM, IlluminaGA, automated pipeline. **b.** BI, IlluminaGA, automated pipeline.

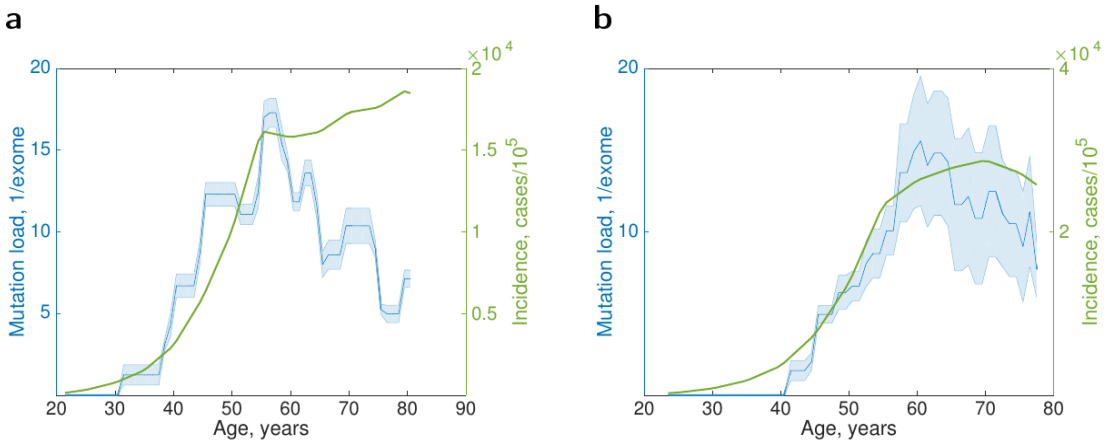

Supplementary Figure 27 | Characteristic somatic mutation load vs. cancer incidence in rectum adenocarcinoma (READ). **a.** Women, BCM, SOLiD. **b.** Men, BCM, SOLiD.

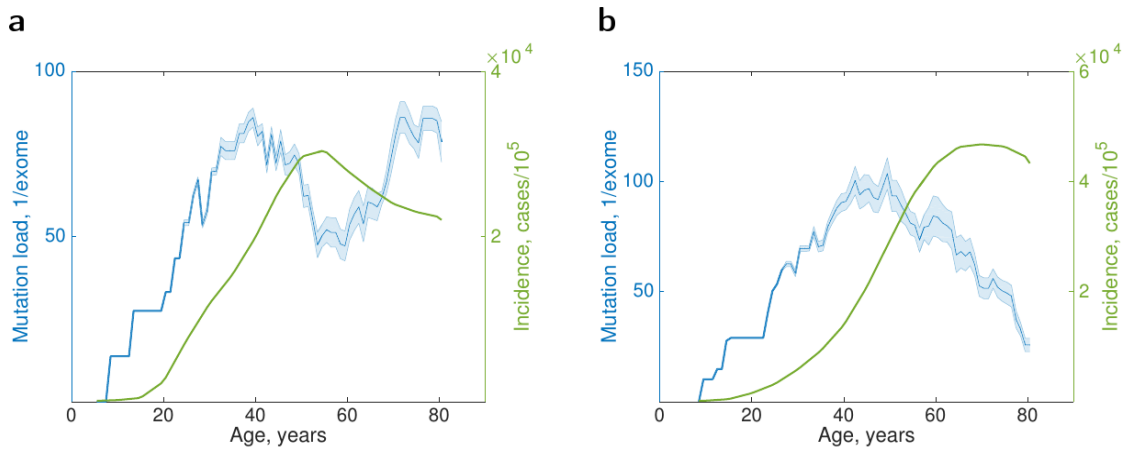

Supplementary Figure 28 | Characteristic somatic mutation load vs. cancer incidence in skin cutaneous melanoma (SKCM). **a.** Women, BCM, IlluminaGA, automated pipeline. **b.** Men, BCM, IlluminaGA, automated pipeline.

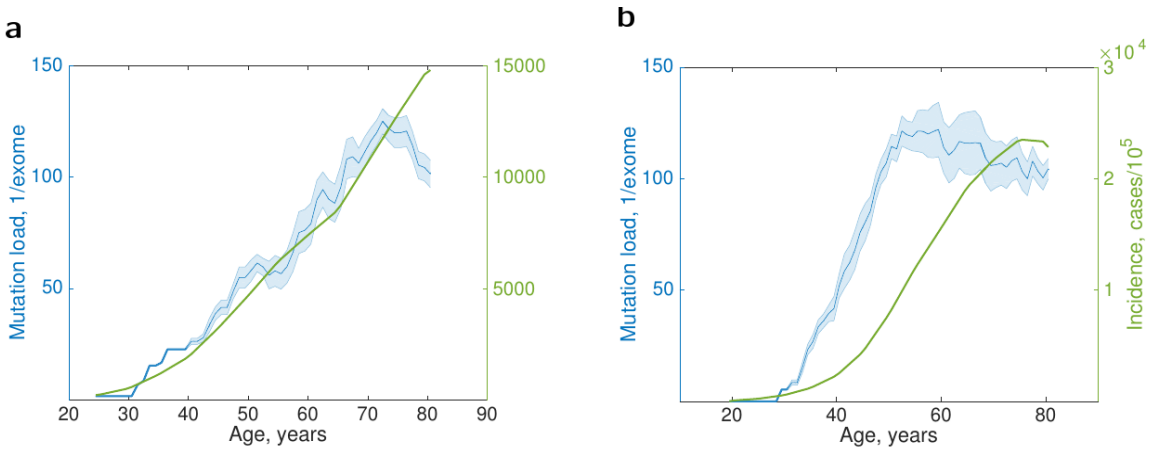

Supplementary Figure 29 | Characteristic somatic mutation load vs. cancer incidence in stomach adenocarcinoma (STAD). **a.** Women, BI, IlluminaGA, automated pipeline. **b.** Men, BI, IlluminaGA, automated pipeline.

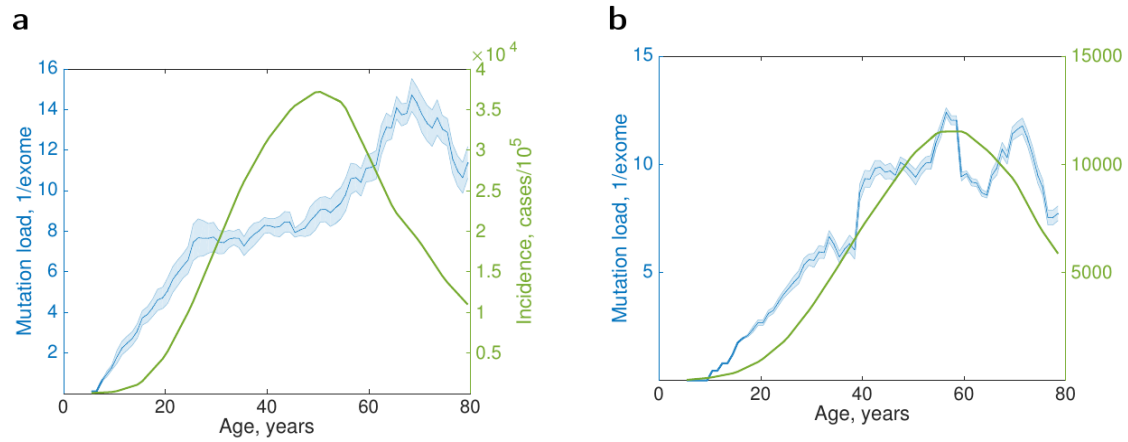

Supplementary Figure 30 | Characteristic somatic mutation load vs. cancer incidence in thyroid carcinoma (THCA). **a.** Women, BCM, IlluminaGA, automated pipeline. **b.** Men, BCM, IlluminaGA, automated pipeline.

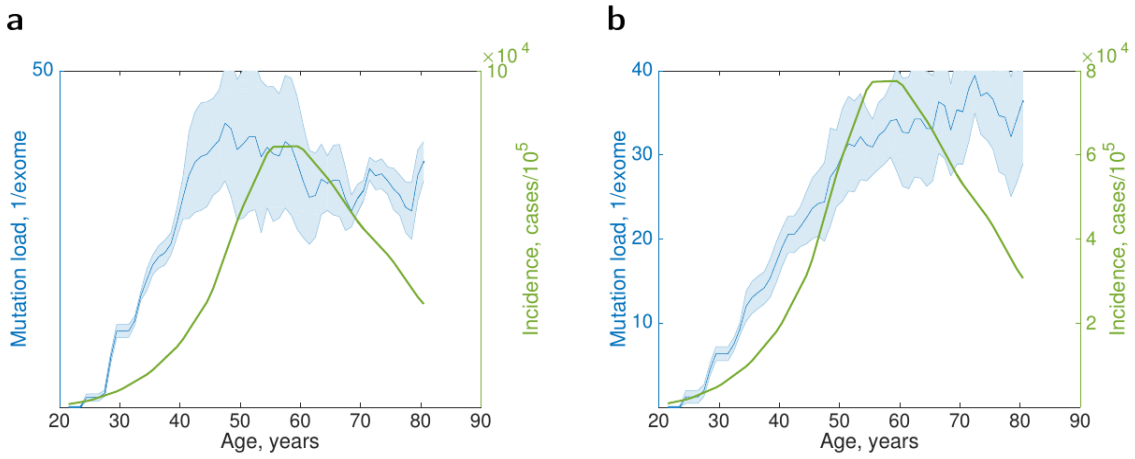

Supplementary Figure 31 | Characteristic somatic mutation load vs. cancer incidence in uterine corpus endometrial carcinoma (UCEC). **a.** BI, IlluminaGA. **b.** WUSM, IlluminaGA.

Growth of cancer incidence with age in different countries

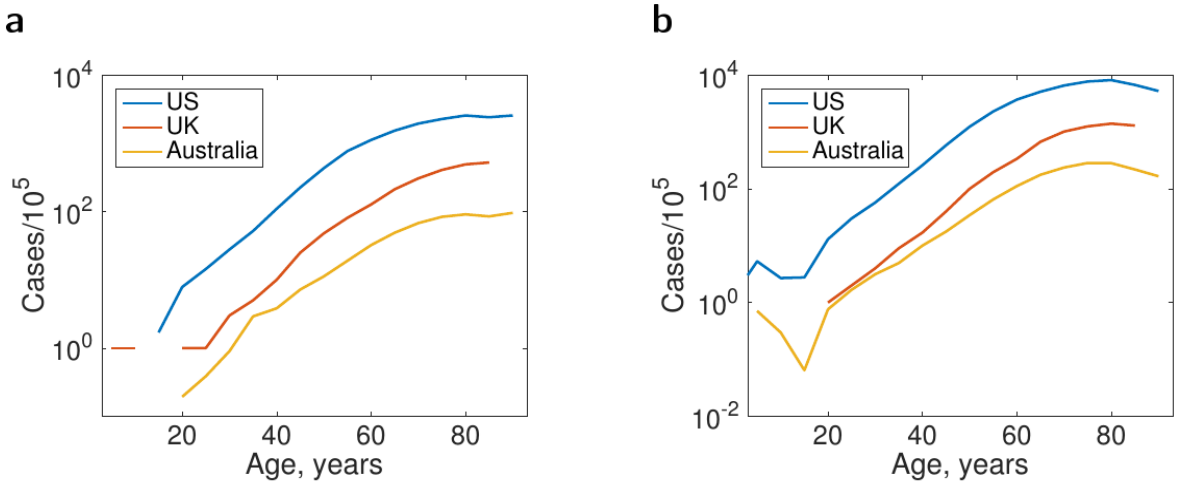

Supplementary Figure 32 | Incidence of bladder cancer in US, UK and Australia, semilog scale. **a.** In women. **b.** In men.

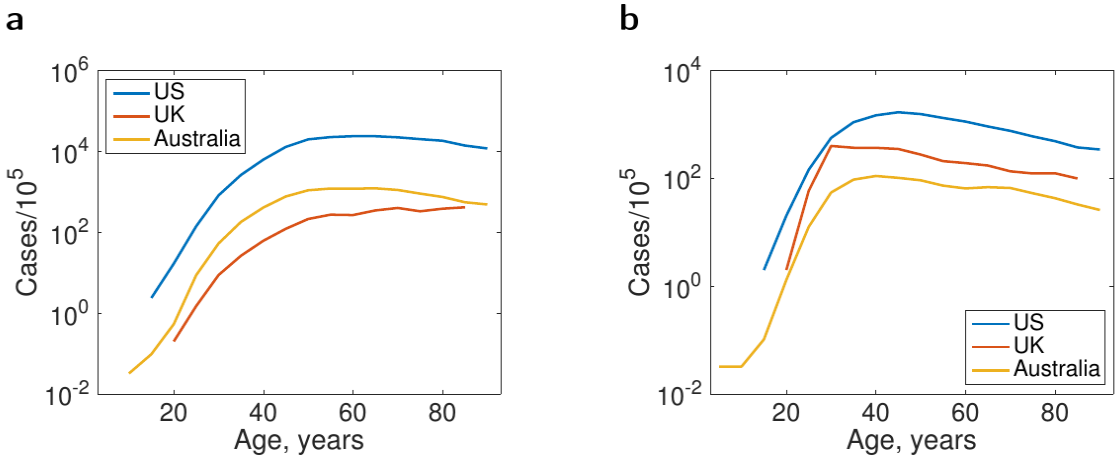

Supplementary Figure 33 | Incidence of breast and cervical cancer in US, UK and Australia, semilog scale. **a.** Breast cancer. **b.** Cervical cancer.

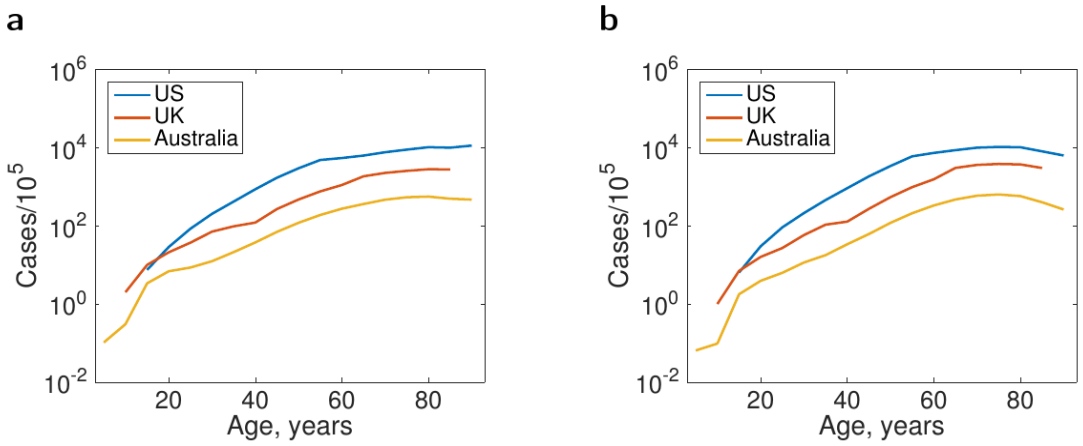

Supplementary Figure 34 | Incidence of colon cancer in US, UK and Australia, semilog scale. **a.** In women. **b.** In men.

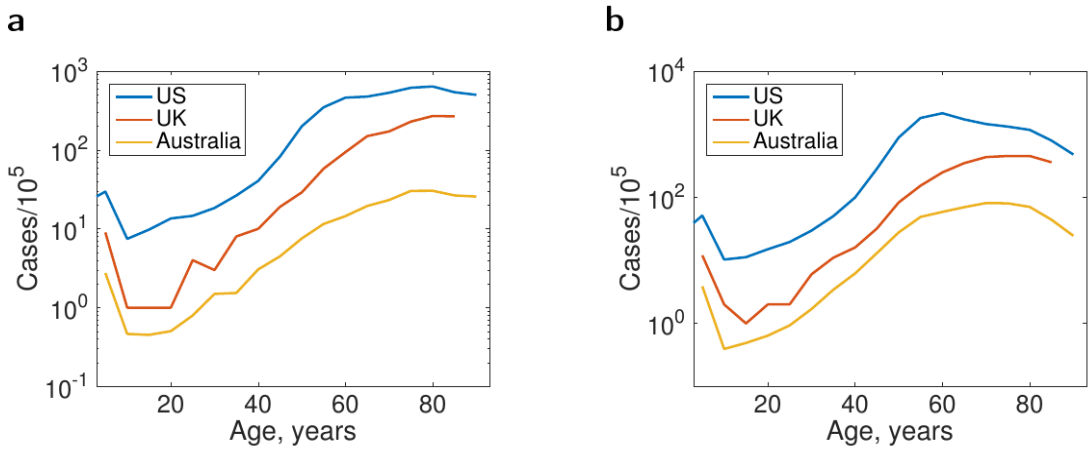

Supplementary Figure 35 | Incidence of liver cancer in US, UK and Australia, semilog scale. **a.** In women. **b.** In men.

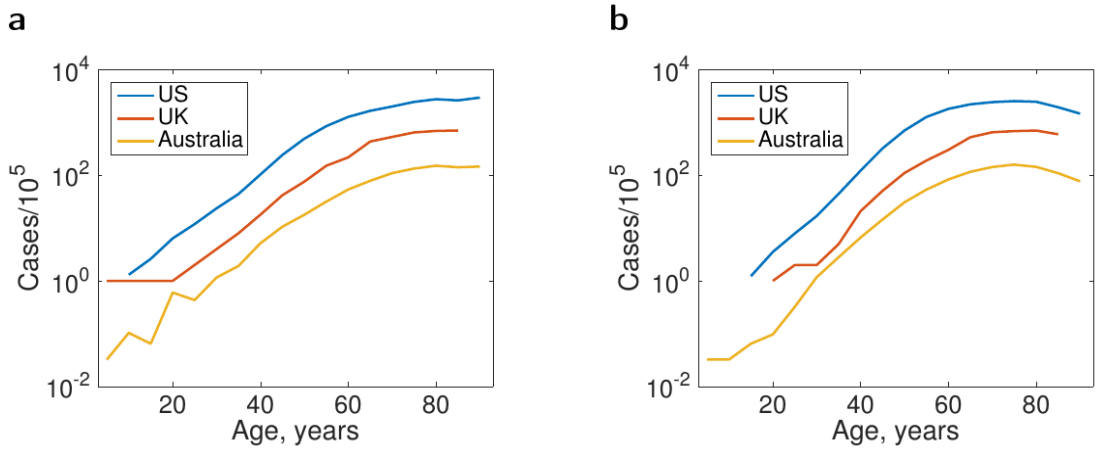

Supplementary Figure 36 | Incidence of pancreatic cancer in US, UK and Australia, semilog scale. **a.** In women. **b.** In men.

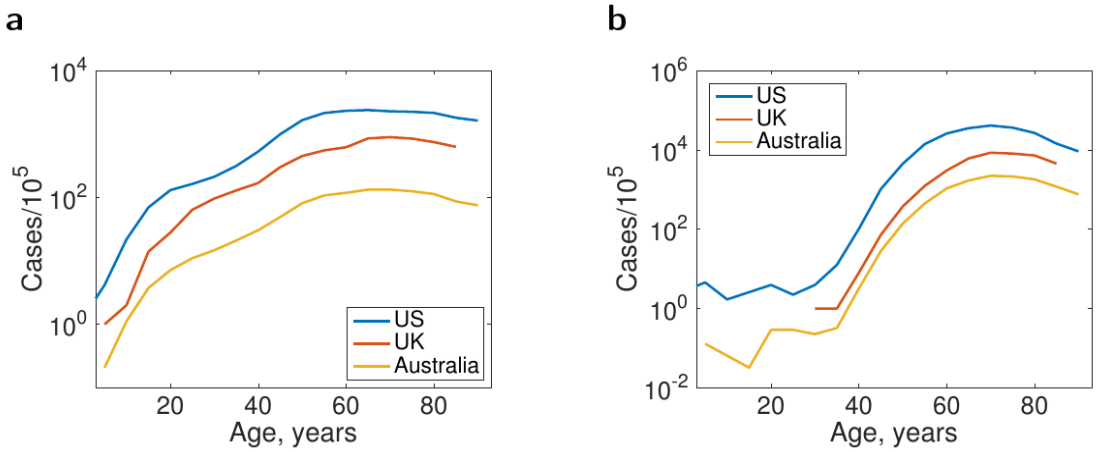

Supplementary Figure 37 | Incidence of ovarian and prostate cancer in US, UK and Australia, semilog scale. **a.** Ovarian cancer. **b.** Prostate cancer.

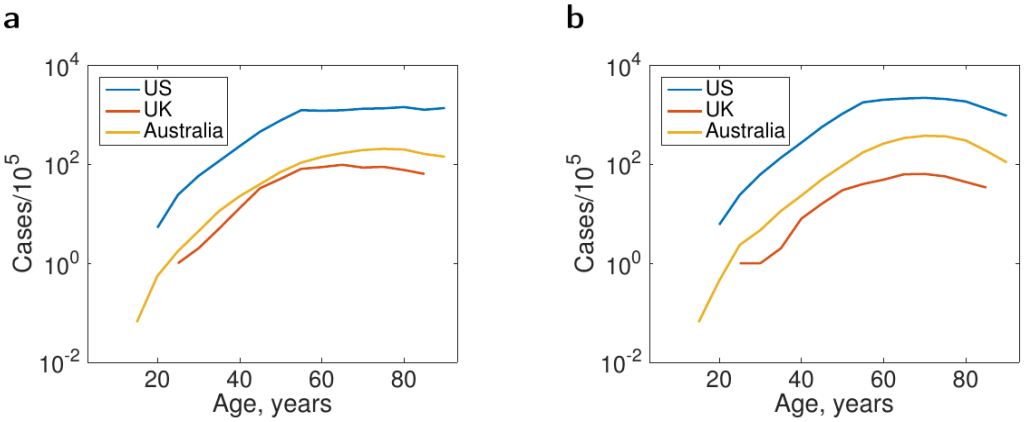

Supplementary Figure 38 | Incidence of rectal cancer in US, UK and Australia, semilog scale. **a.** In women. **b.** In men.

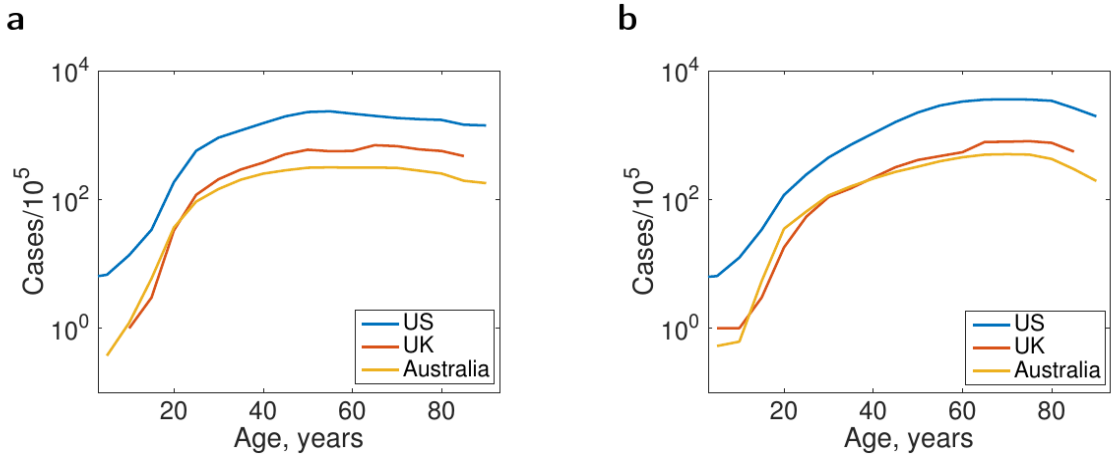

Supplementary Figure 39 | Incidence of skin melanoma in US, UK and Australia, semilog scale. **a.** In women. **b.** In men.

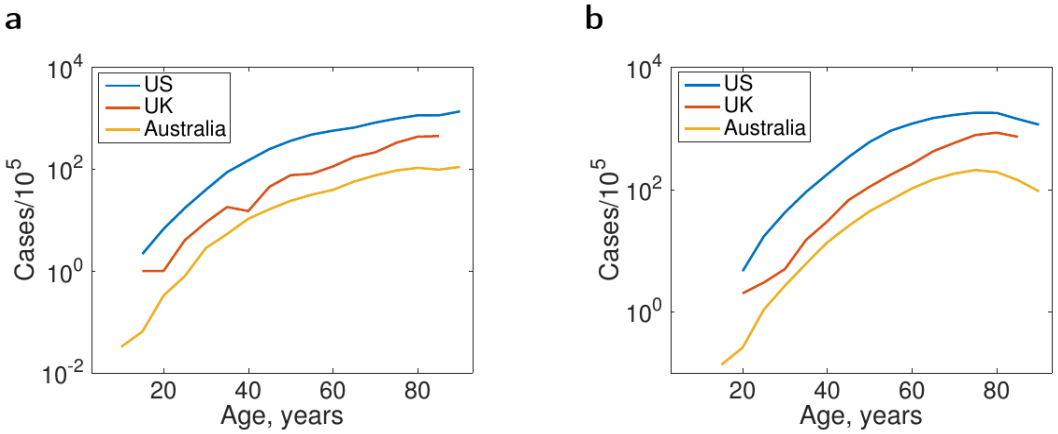

Supplementary Figure 40 | Incidence of stomach melanoma in US, UK and Australia, semilog scale. **a.** In women. **b.** In men.

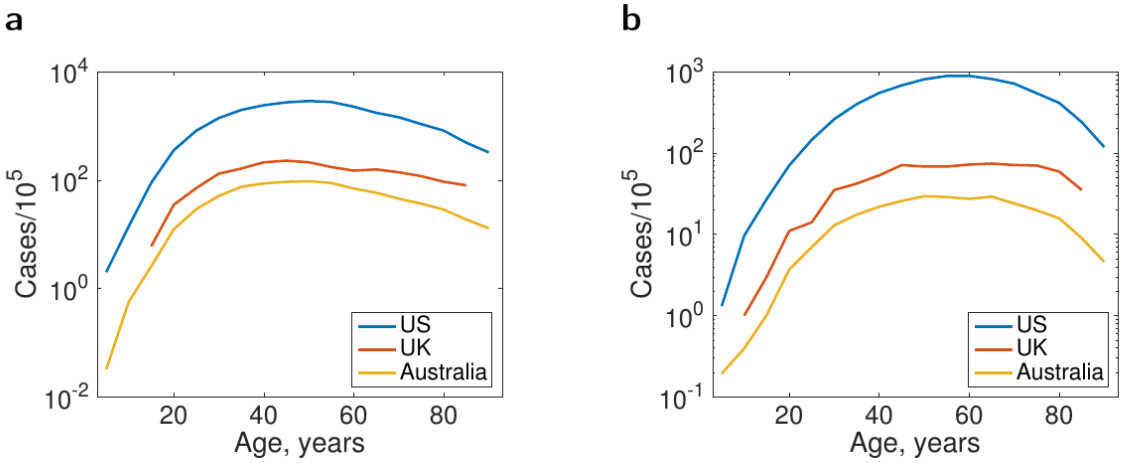

Supplementary Figure 41 | Incidence of thyroid cancer in US, UK and Australia, semilog scale. **a.** In women. **b.** In men.

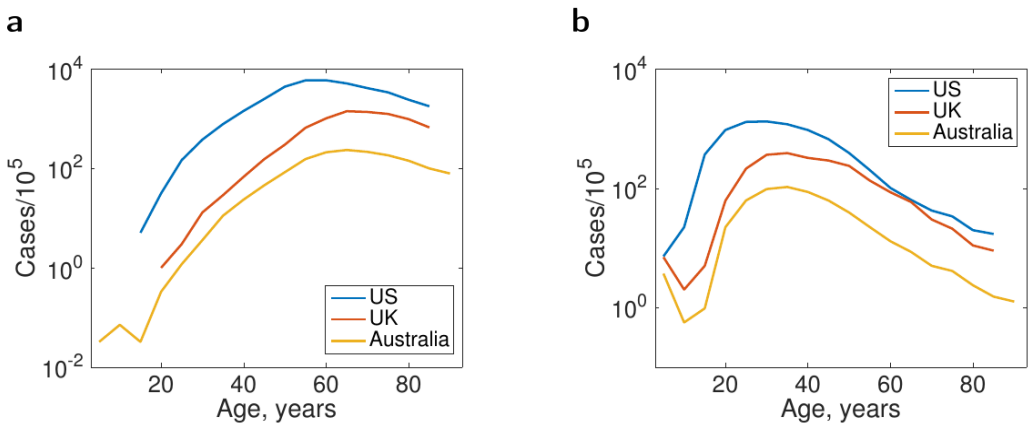

Supplementary Figure 42 | Incidence of uterine and testicular cancer in US, UK and Australia, semilog scale. **a.** Uterine cancer. **b.** Testicular cancer.

Mutation counting in whole genomes

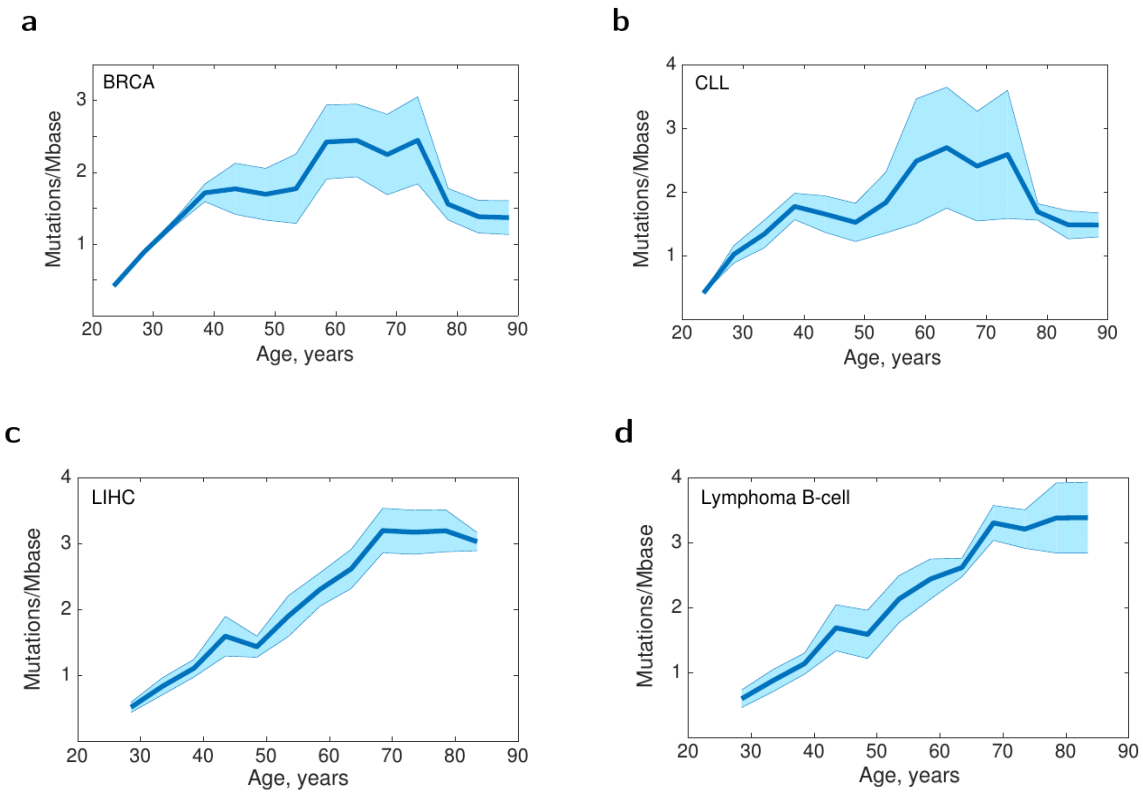

Supplementary Figure 43 | Behavior of mutational load with age in whole genomes. **a.** Breast invasive carcinoma. **b.** Chronic lymphocytic leukemia. **c.** Liver hepatic carcinoma. **d.** B-cell lymphoma.

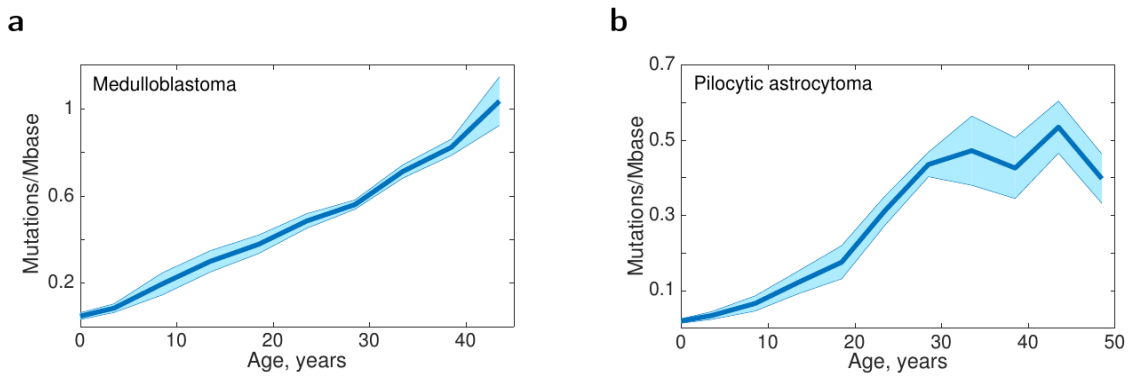

Supplementary Figure 44 | Behavior of mutational load with age in whole genomes. **a.** Medulloblastoma. **b.** Pilocytic astrocytoma.

Examples of chronological age distributions for samples covered by TCGA

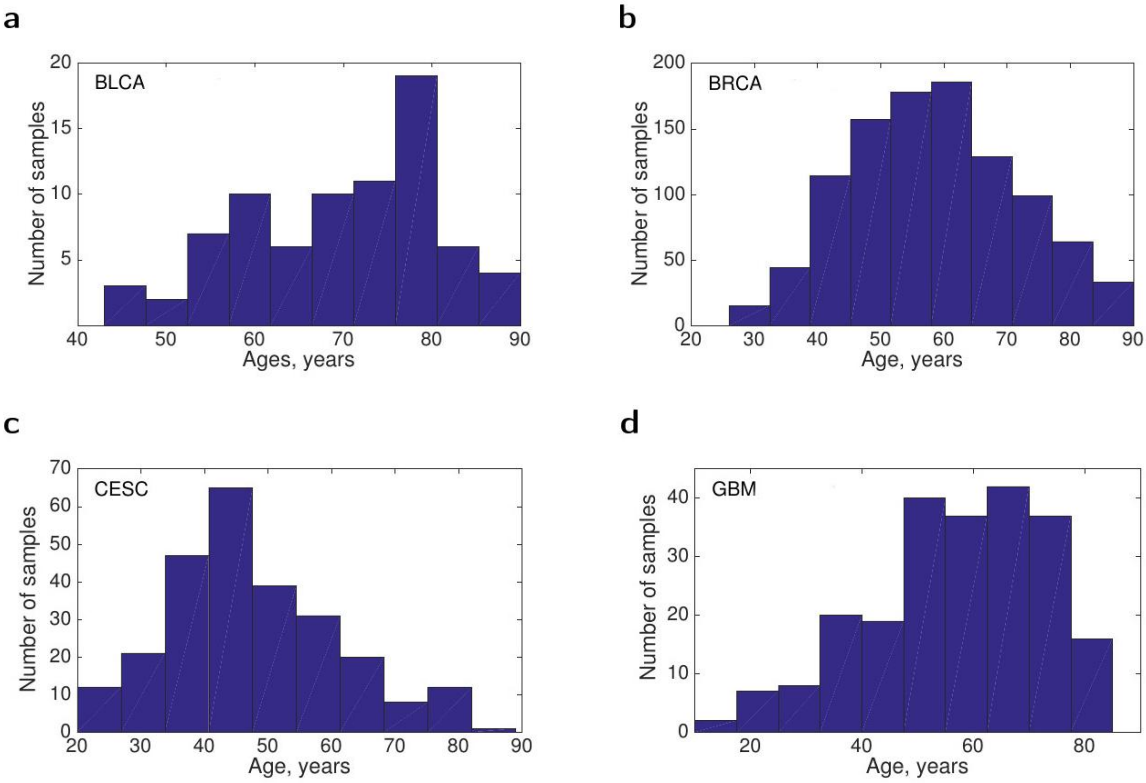

Supplementary Figure 45 | Chronological age distributions for samples covered by TCGA atlas, women. **a.** Bladder adenocarcinoma, BI, automated pipeline. **b.** Breast invasive carcinoma, WUSM, curated pipeline. **c.** Cervical squamous cell carcinoma, BSGSC, IlluminaHiSeq, automated pipeline. **d.** Glioblastoma, BI, Illumina pipeline.

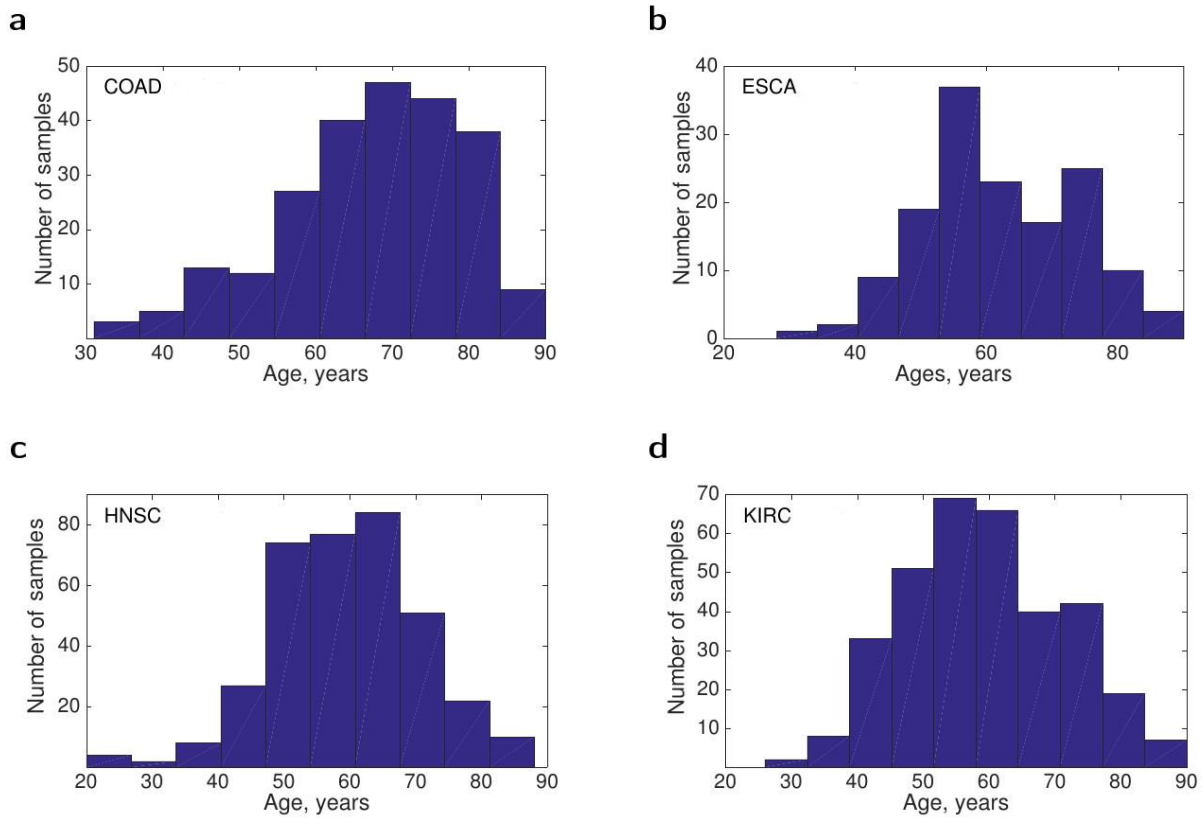

Supplementary Figure 46 | Chronological age distributions for samples covered by TCGA atlas, men. **a.** Colon adenocarcinoma, BCM, IlluminaGA. **b.** Esophageal adenocarcinoma, BCGSC, IlluminaHiSeq, automated pipeline. **c.** Head and neck squamous cell carcinoma. BI, IlluminaGA. **d.** Kidney renal clear cell carcinoma, BI, Illumina, automated pipeline.

Relative weights of different indels and SNVs in the age-correlated somatic mutation load pattern

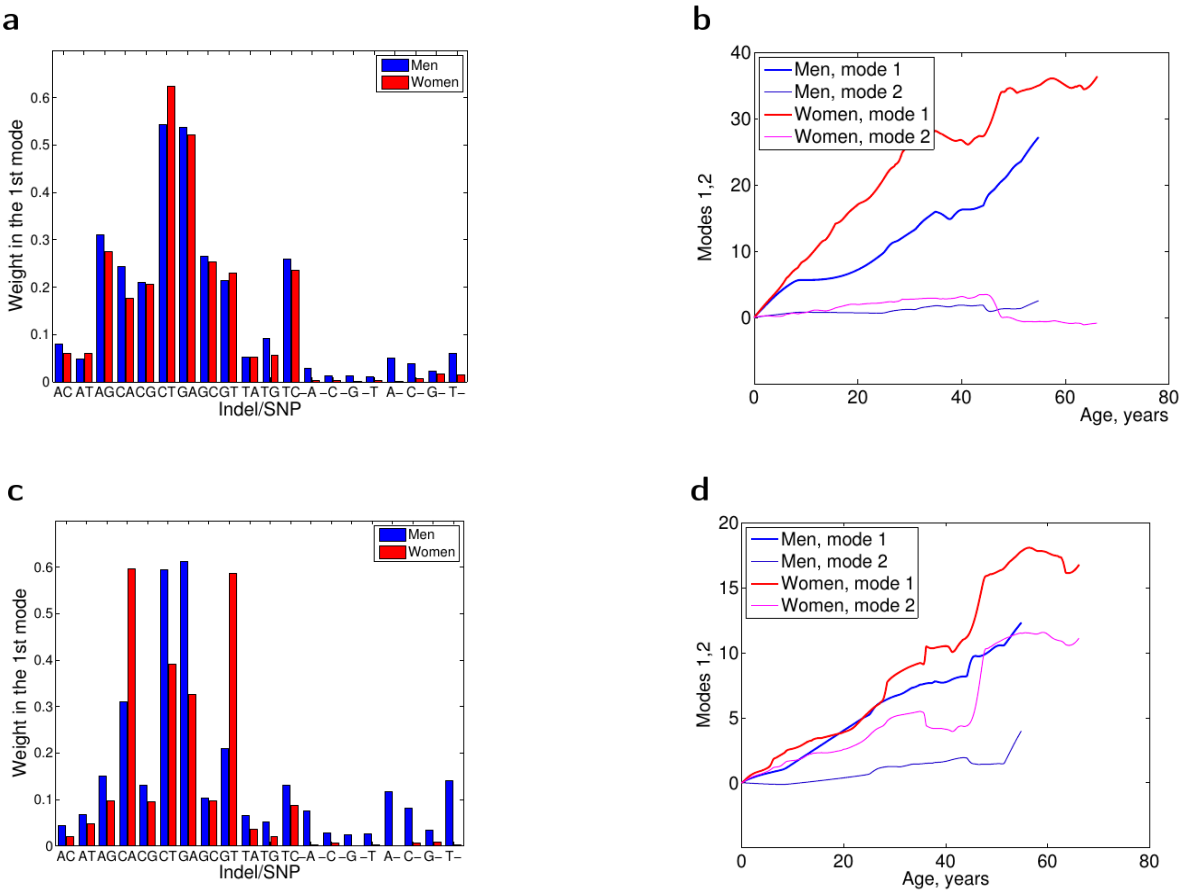

Supplementary Figure 47 | Modal structure of somatic mutation load in adrenocortical carcinoma (ACC). **a.** BCM, IlluminaGA DNASeq, automated pipeline; relative weights of different SNVs and indels. **b.** BCM, IlluminaGA DNASeq, automated pipeline; count estimation using projection on the leading pattern. **c.** BCM, IlluminaGA DNASeq, curated pipeline relative weights of different SNVs and indels. **d.** BCM, IlluminaGA DNASeq, automated pipeline; count estimation using projection on the leading pattern.

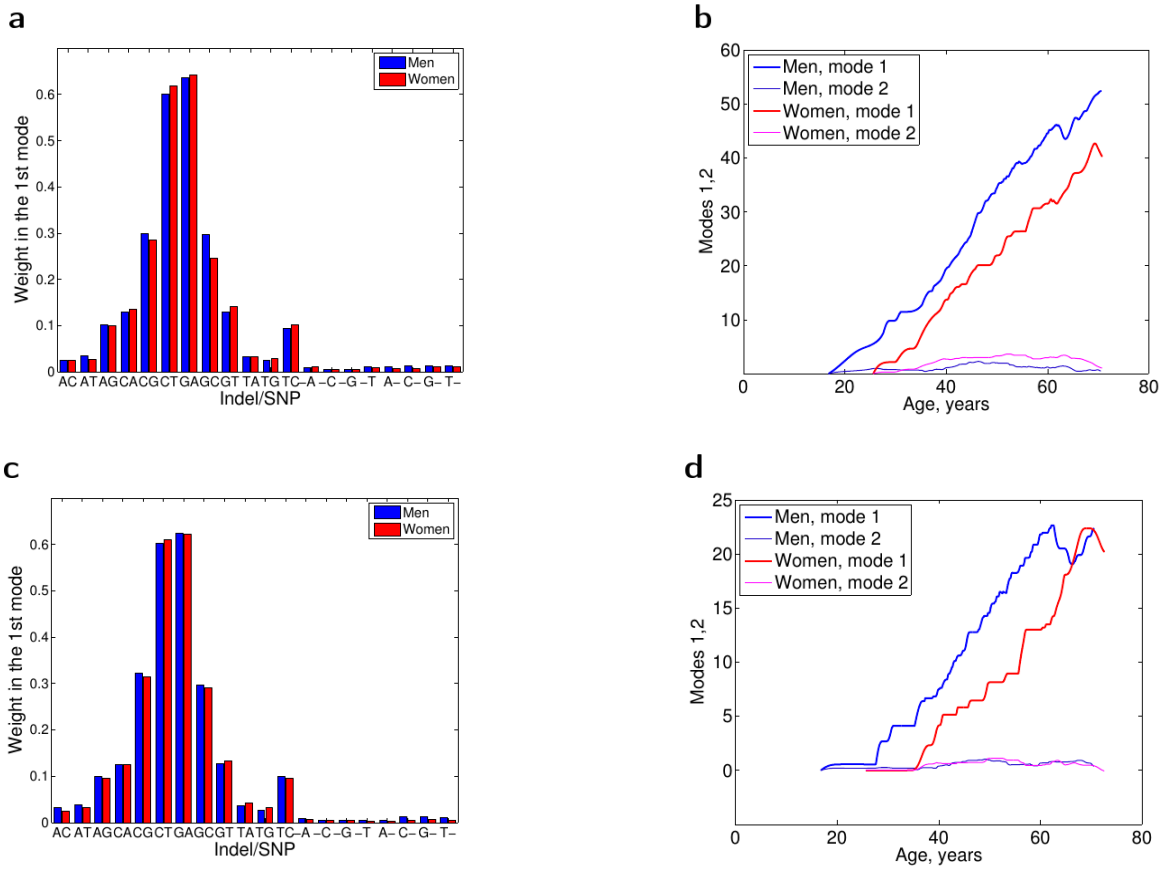

Supplementary Figure 48 | Modal structure of somatic mutation load in bladder urothelial carcinoma (BLCA). **a.** BI, IlluminaGA DNASeq, automated pipeline; relative weights of different SNVs and indels. **b.** BI, IlluminaGA DNASeq, automated pipeline; count estimation using projection on the leading pattern. **c.** BI, IlluminaGA DNASeq, curated pipeline; relative weights of different SNVs and indels. **d.** BI, IlluminaGA DNASeq, curated pipeline; count estimation using projection on the leading pattern.

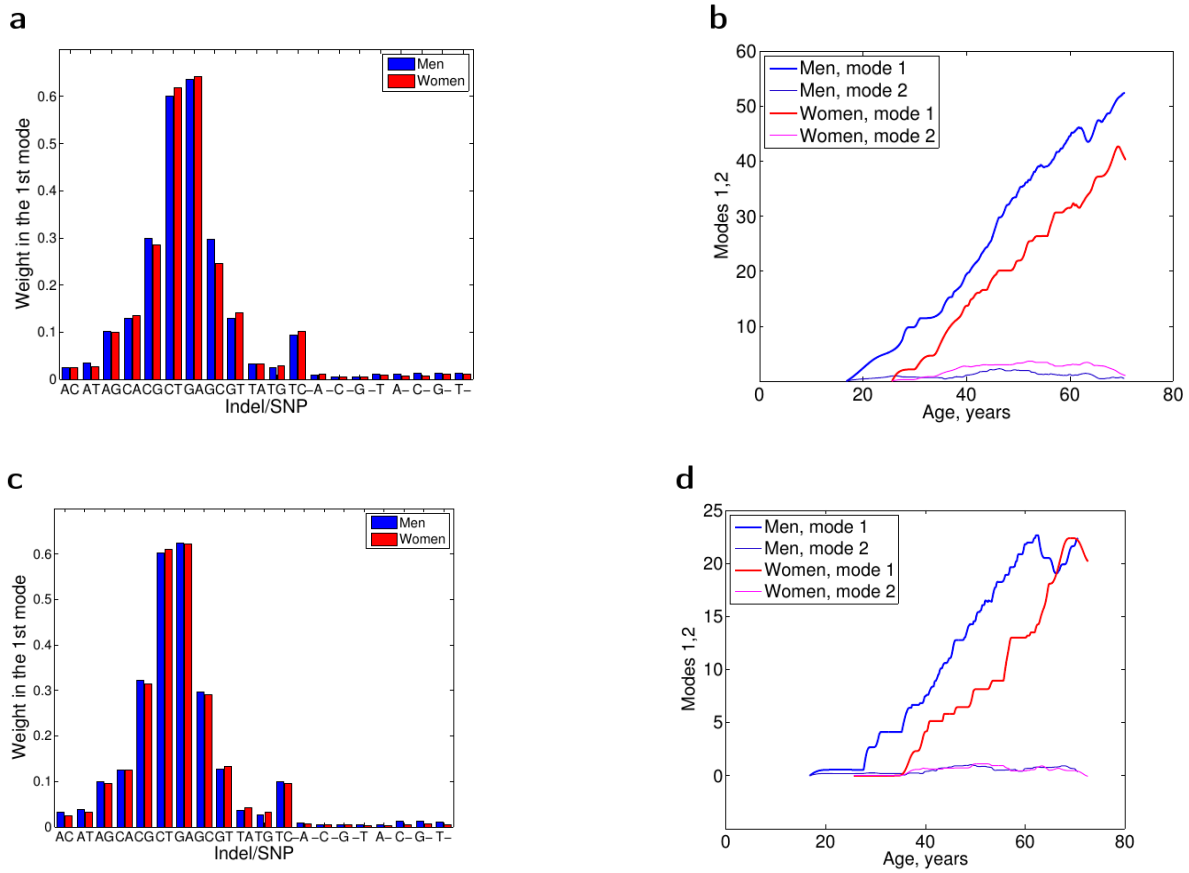

Supplementary Figure 49 | Modal structure of somatic mutation load in breast invasive carcinoma (BRCA). **a.** WUSM, IlluminaGA DNASeq, curated pipeline; relative weights of different SNVs and indels. **b.** WUSM, IlluminaGA DNASeq, curated pipeline; count estimation using projection on the leading pattern. **c.** WUSM, IlluminaGA DNASeq; relative weights of different SNVs and indels. **d.** WUSM, IlluminaGA DNASeq; count estimation using projection on the leading pattern.

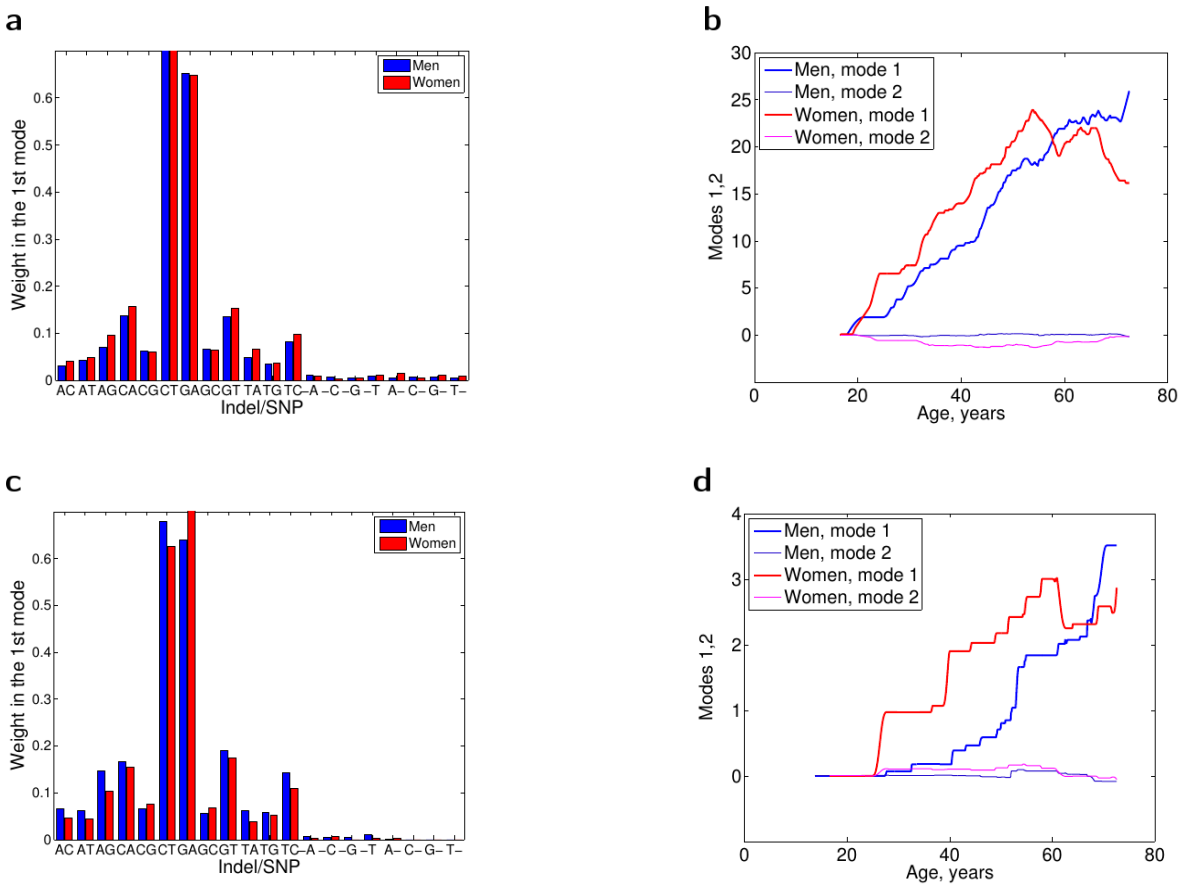

Supplementary Figure 50 | Modal structure of somatic mutation load in colon adenocarcinoma (COAD). **a.** BCM, IlluminaGA DNASeq; relative weights of different SNVs and indels. **b.** BCM, IlluminaGA DNASeq; count estimation using projection on the leading pattern. **c.** BCM, SOLiD DNASeq; relative weights of different SNVs and indels. **d.** BCM, SOLiD DNASeq; count estimation using projection on the leading pattern.

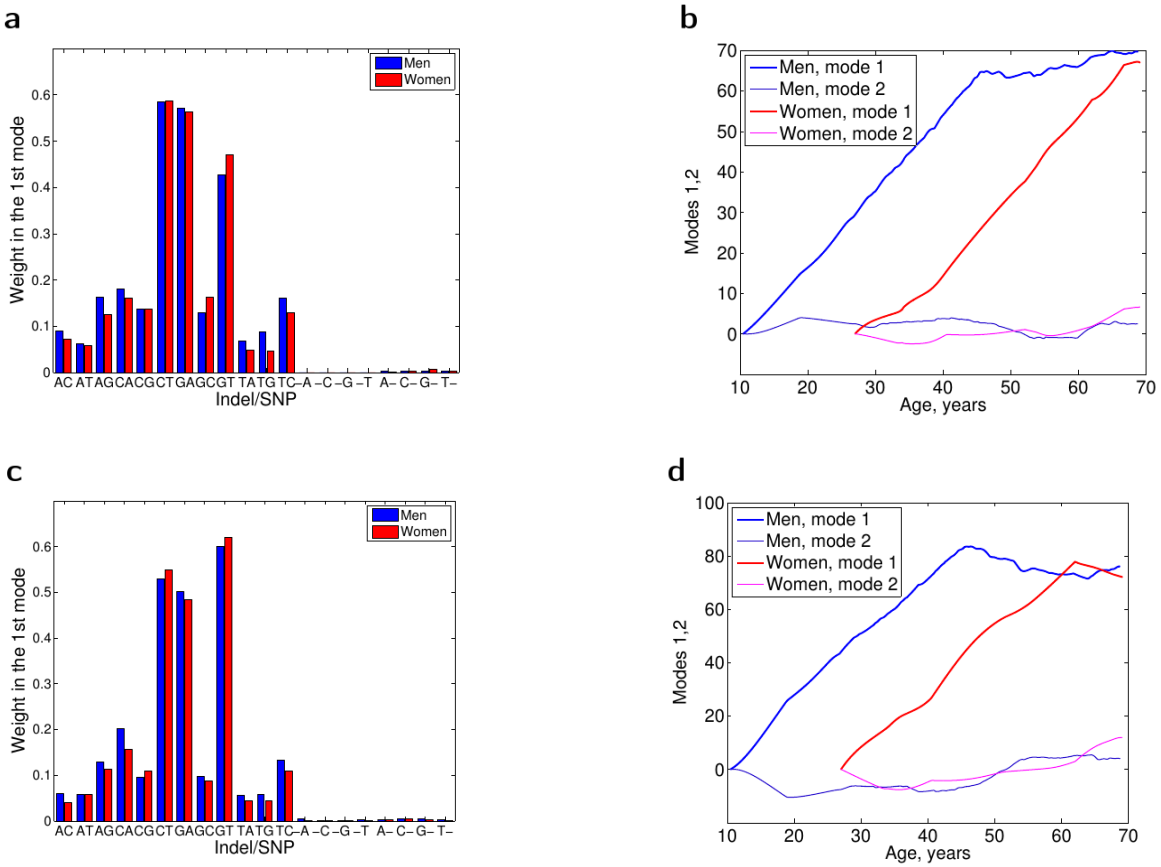

Supplementary Figure 51 | Modal structure of somatic mutation load in esophageal carcinoma (ESCA). **a.** BCGSC, IlluminaHiSeq DNASeq, automated pipeline; relative weights of different SNVs and indels. **b.** BCGSC, IlluminaHiSeq DNASeq, automated pipeline; count estimation using projection on the leading pattern. **c.** BCM, IlluminaGA DNASeq, automated pipeline; relative weights of different SNVs and indels. **d.** BCM, IlluminaGA DNASeq, automated pipeline; count estimation using projection on the leading pattern.

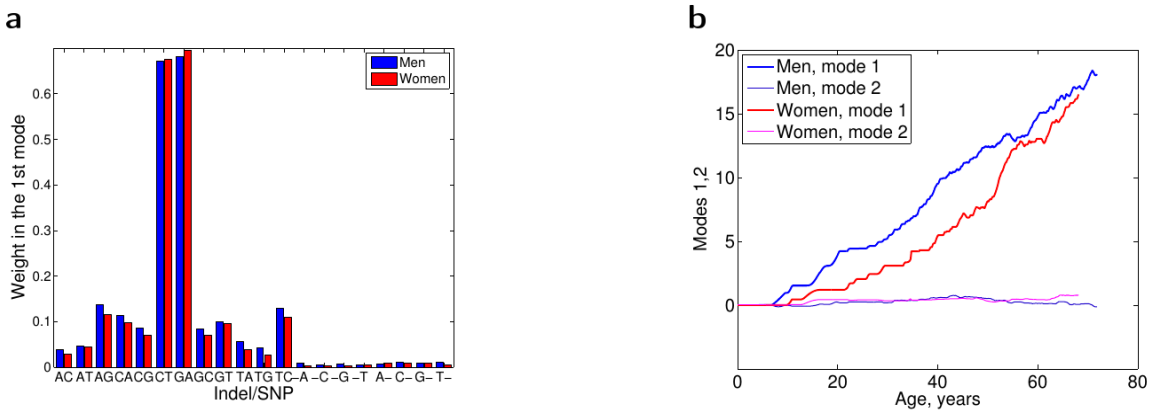

Supplementary Figure 52 | Modal structure of somatic mutation load in glioblastoma multiforme (GBM). **a.** BI, IlluminaGA DNASeq; relative weights of different SNVs and indels. **b.** BI, IlluminaGA DNASeq; count estimation using projection on the leading pattern.

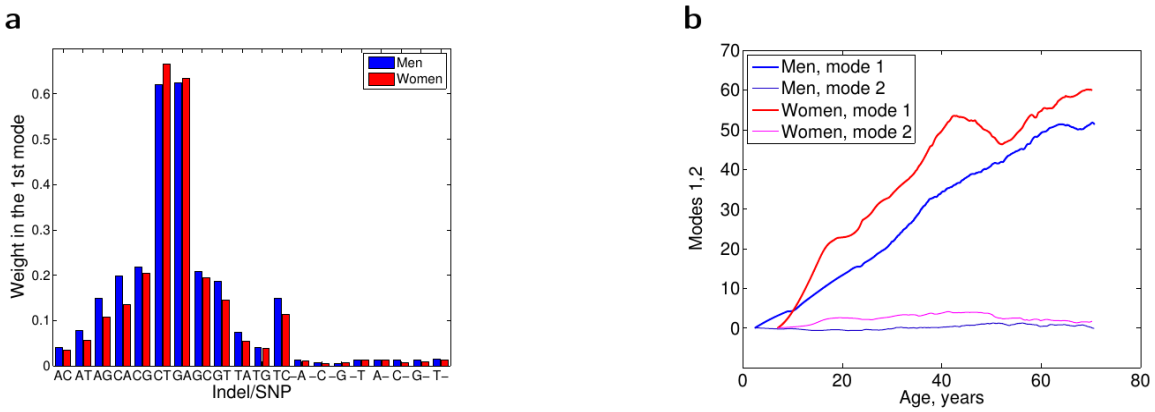

Supplementary Figure 53 | Modal structure of somatic mutation load in head and neck squamous cell carcinoma (HNSC). **a.** BI, IlluminaGA DNASeq, automated pipeline; relative weights of different SNVs and indels. **b.** BI, IlluminaGA DNASeq, automated pipeline; count estimation using projection on the leading pattern.

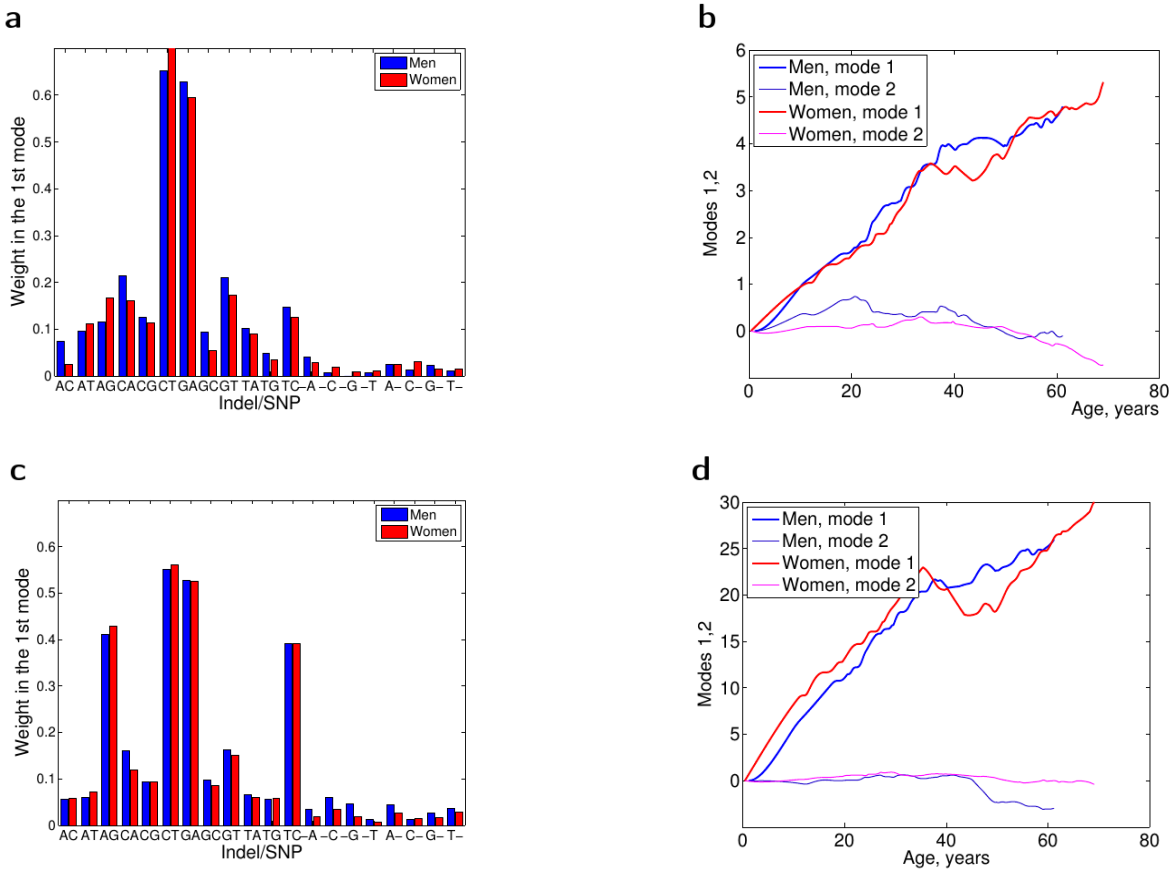

Supplementary Figure 54 | Modal structure of somatic mutation load in kidney chromophobe (KICH). **a.** BCM, IlluminaGA DNASeq, automated pipeline; relative weights of different SNVs and indels. **b.** BCM, IlluminaGA DNASeq, automated pipeline; count estimation using projection on the leading pattern. **c.** BCM, mixed IlluminaGA and SOLiD, curated pipeline; relative weights of different SNVs and indels. **d.** BCM, mixed IlluminaGA and SOLiD, curated pipeline; count estimation using projection on the leading pattern.

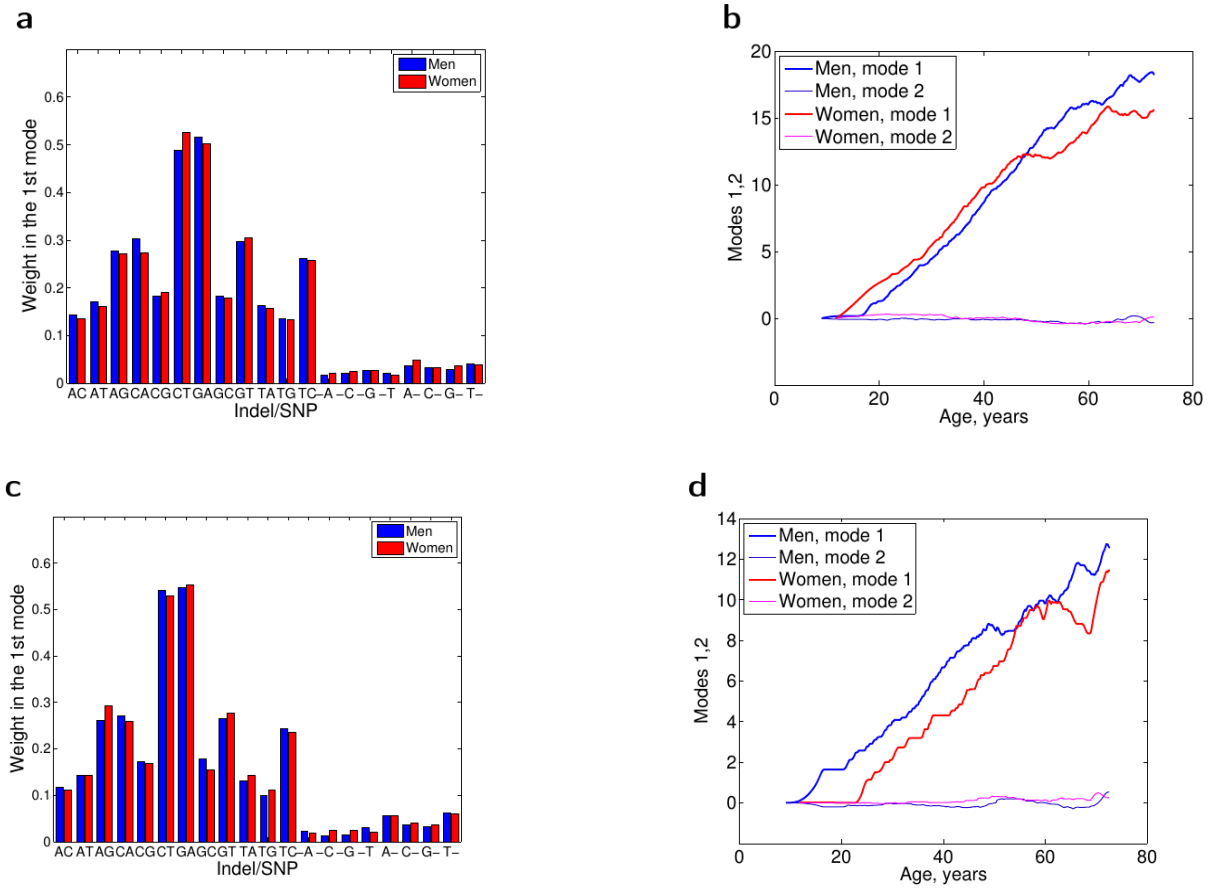

Supplementary Figure 55 | Modal structure of somatic mutation load in kidney renal clear cell carcinoma (KIRC). **a.** BCM, mixed IlluminaGA and SOLiD; relative weights of different SNVs and indels. **b.** BCM, mixed IlluminaGA and SOLiD; count estimation using projection on the leading pattern. **c.** BI, IlluminaGA DNASeq, automated pipeline; relative weights of different SNVs and indels. **d.** BI, IlluminaGA DNASeq, automated pipeline; count estimation using projection on the leading pattern.

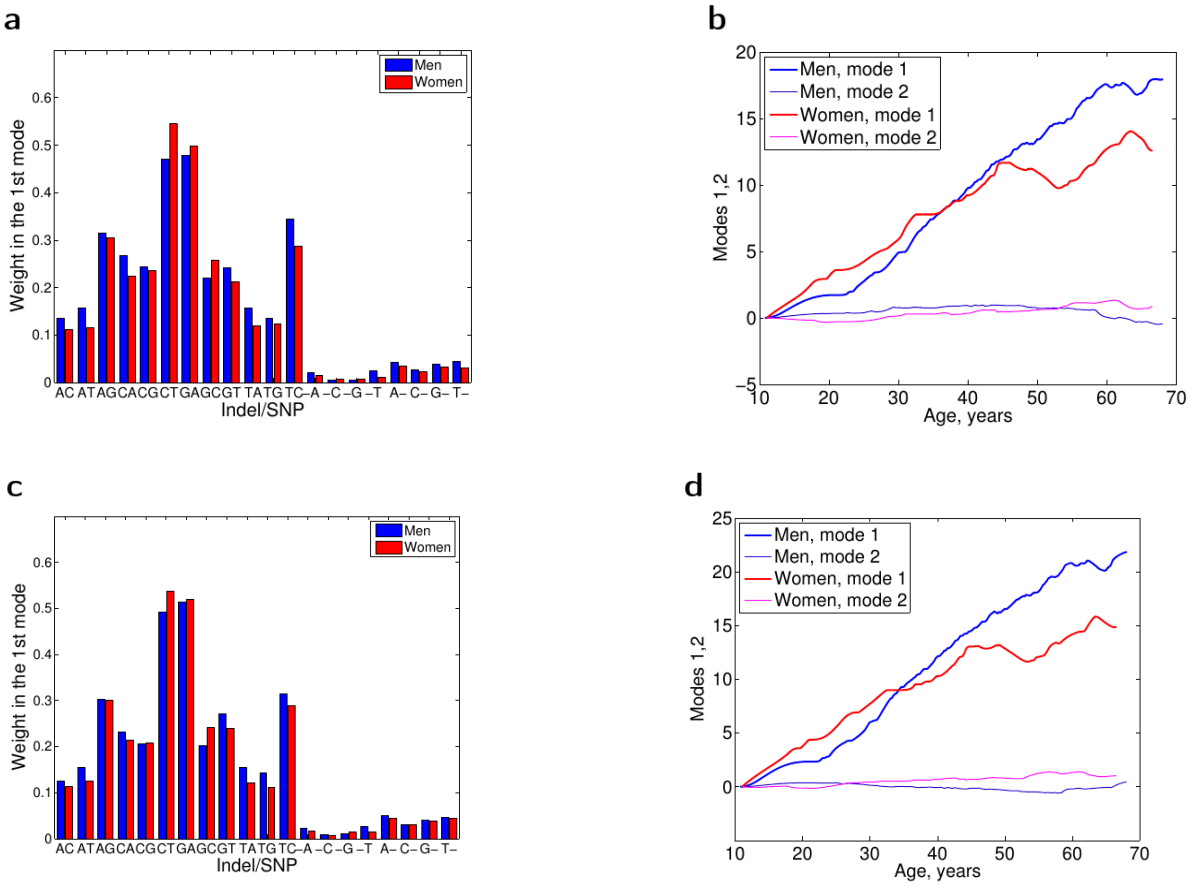

Supplementary Figure 56 | Modal structure of somatic mutation load in kidney renal papillary cell carcinoma (KIRP). **a.** BCM, IlluminaGA DNASeq, curated pipeline; relative weights of different SNVs and indels. **b.** BCM, IlluminaGA DNASeq, curated pipeline; count estimation using projection on the leading pattern. **c.** BCM, mixed IlluminaGA and SOLiD, curated pipeline; relative weights of different SNVs and indels. **d.** BCM, mixed IlluminaGA and SOLiD, curated pipeline; count estimation using projection on the leading pattern.

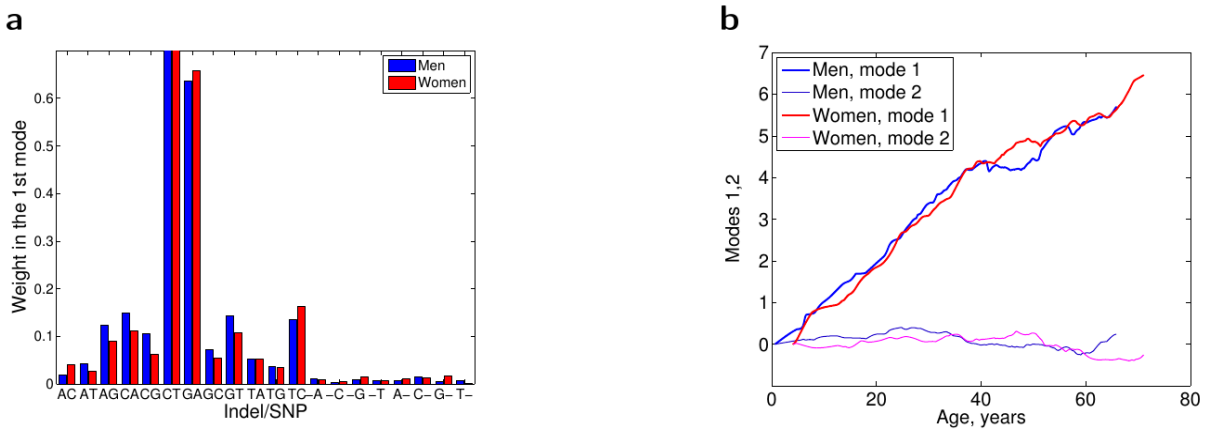

Supplementary Figure 57 | Modal structure of somatic mutation load in acute myeloid leukemia (LAML). **a.** WUSM, IlluminaGA DNASeq; relative weights of different SNVs and indels. **b.** WUSM, IlluminaGA DNASeq; count estimation using projection on the leading pattern.

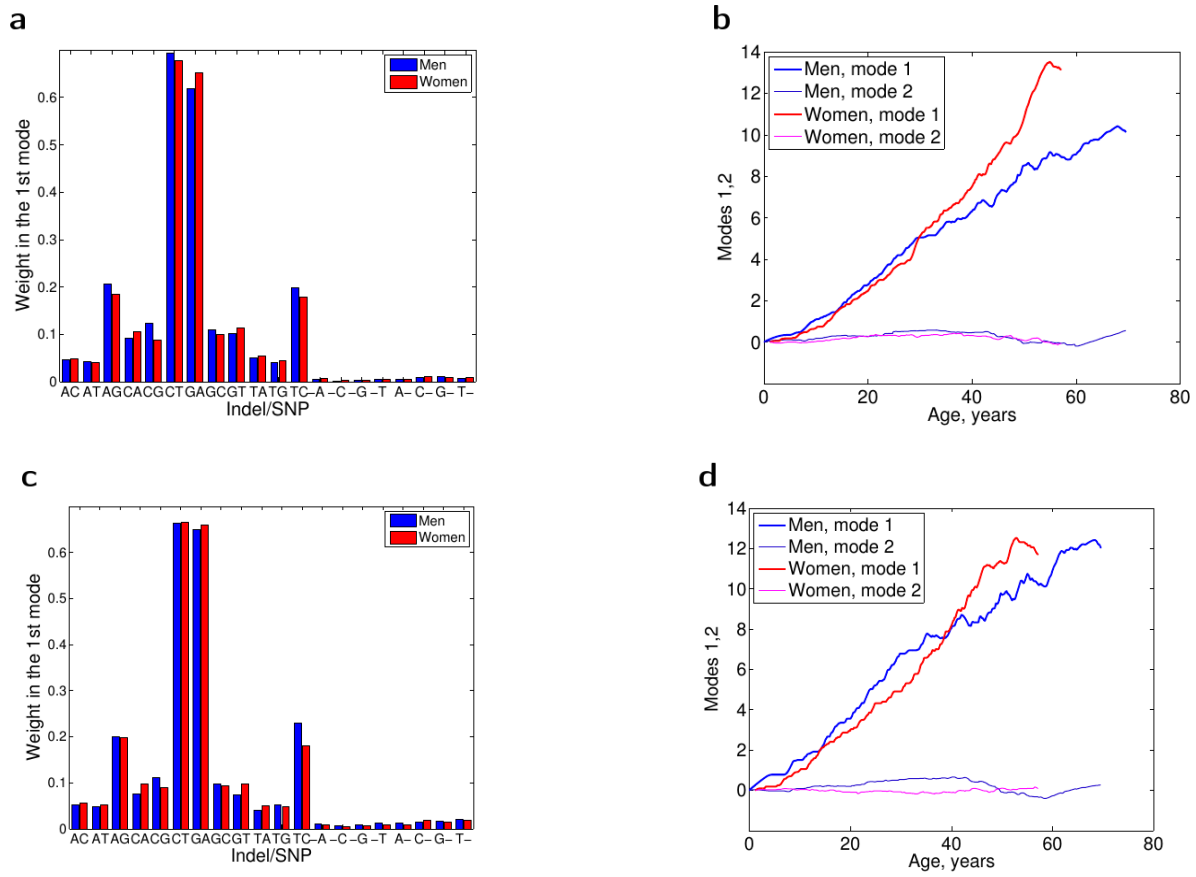

Supplementary Figure 58 | Modal structure of somatic mutation load in brain lower grade glioma (LGG). **a.** BCM, IlluminaGA DNASeq, automated pipeline; relative weights of different SNVs and indels. **b.** BCM, IlluminaGA DNASeq, automated pipeline; count estimation using projection on the leading pattern. **c.** BI, IlluminaGA DNASeq; relative weights of different SNVs and indels. **d.** BI, IlluminaGA DNASeq; count estimation using projection on the leading pattern.

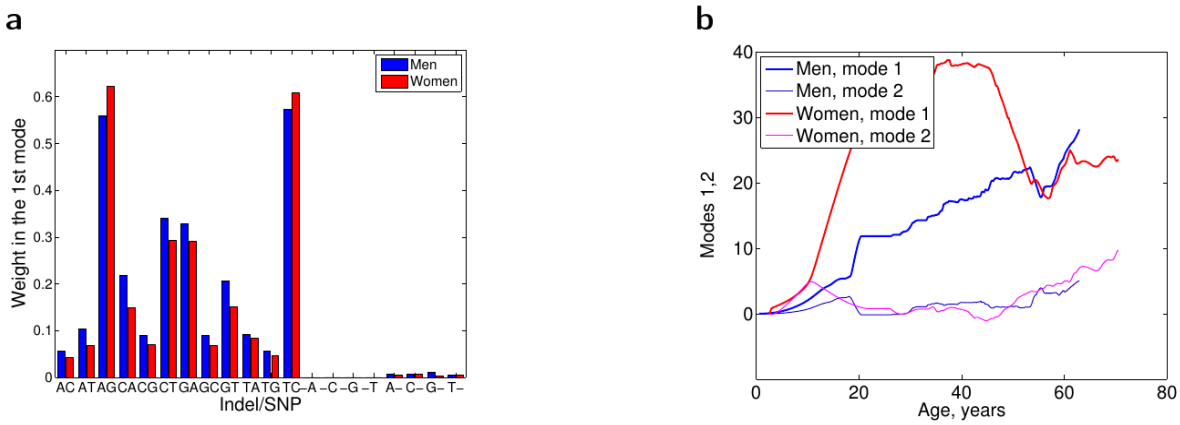

Supplementary Figure 59 | Modal structure of somatic mutation load in liver hepatocellular carcinoma (LIHC). **a.** BCGSC, IlluminaHiSeq DNASeq, automated pipeline; relative weights of different SNVs and indels. **b.** BCGSC, IlluminaHiSeq DNASeq, automated pipeline; count estimation using projection on the leading pattern.

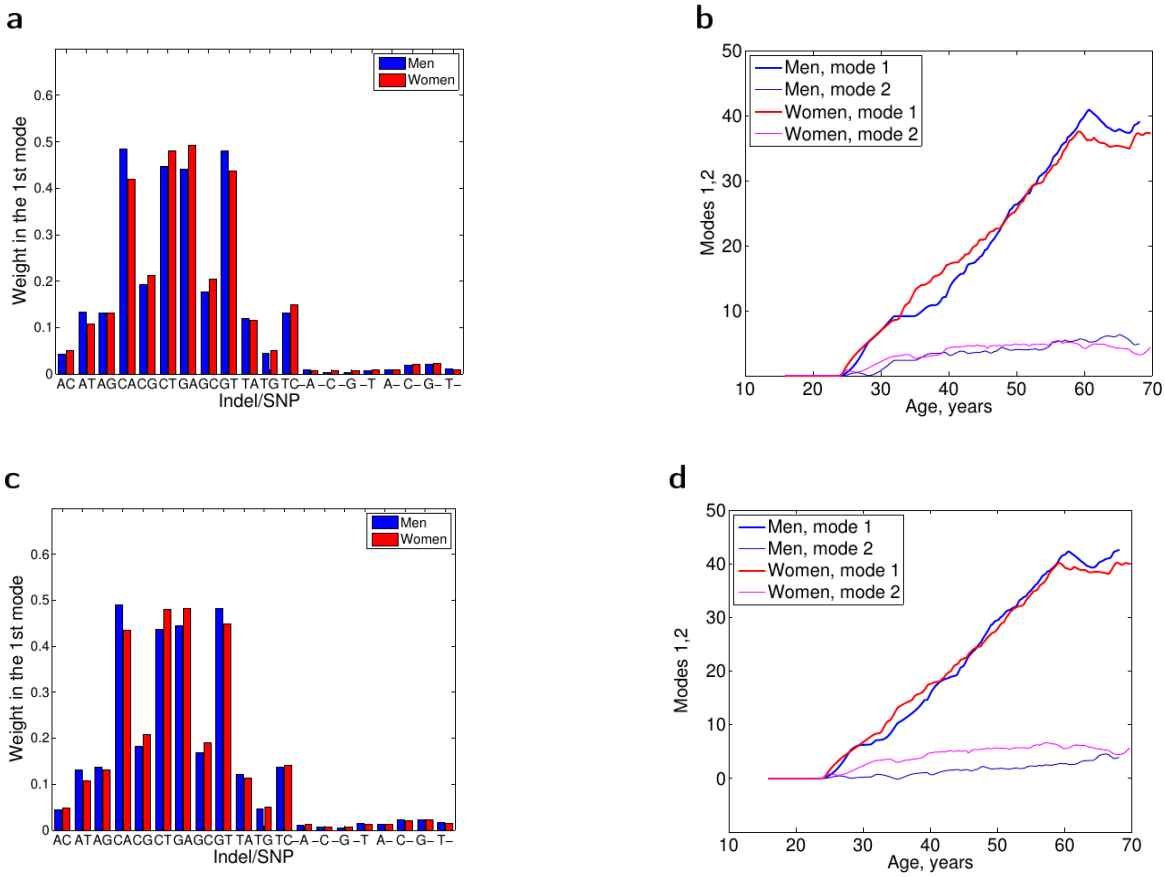

Supplementary Figure 60 | Modal structure of somatic mutation load in lung adenocarcinoma (LUAD). **a.** BI, IlluminaGA DNASeq; relative weights of different SNVs and indels. **b.** BI, IlluminaGA DNASeq; count estimation using projection on the leading pattern. **c.** BI, IlluminaGA DNASeq, automated pipeline; relative weights of different SNVs and indels. **d.** BI, IlluminaGA DNASeq, automated pipeline; count estimation using projection on the leading pattern.

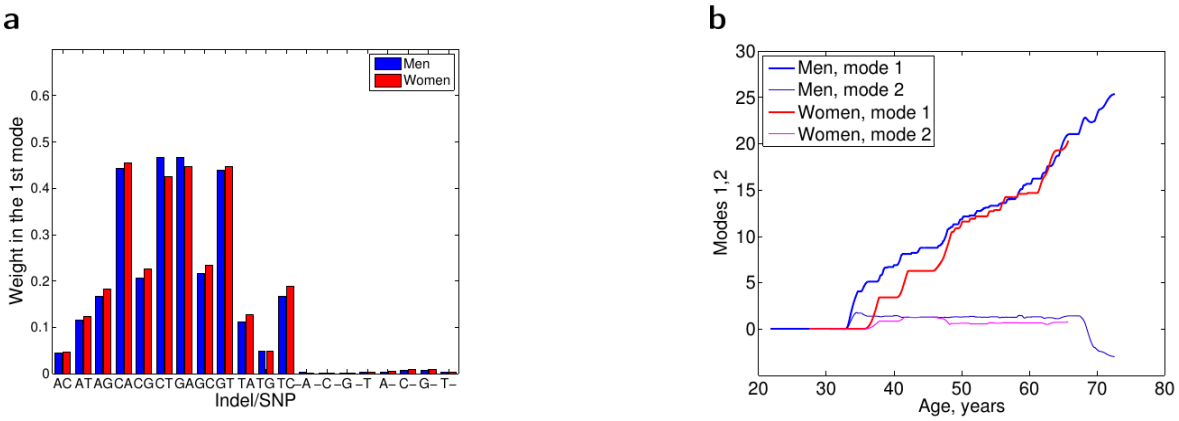

Supplementary Figure 61 | Modal structure of somatic mutation load in lung squamous cell carcinoma (LUSC). **a.** BI, IlluminaGA DNASeq; relative weights of different SNVs and indels. **b.** BI, IlluminaGA DNASeq; count estimation using projection on the leading pattern.

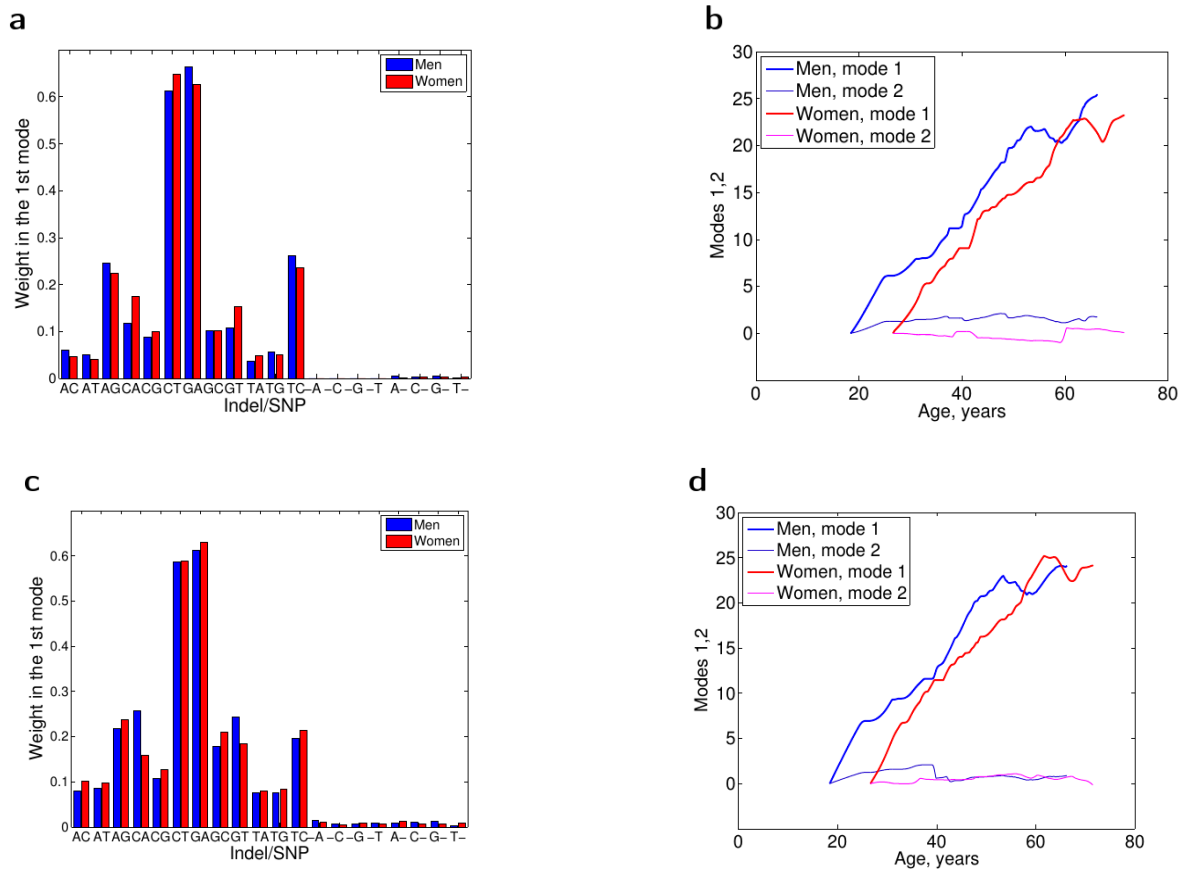

Supplementary Figure 62 | Modal structure of somatic mutation load in lung adenocarcinoma (LUAD). **a.** BCGSC, IlluminaHiSeq DNASeq, automated pipeline; relative weights of different SNVs and indels. **b.** BCGSC, IlluminaHiSeq DNASeq, automated pipeline; count estimation using projection on the leading pattern. **c.** BCM, IlluminaGA DNASeq, automated pipeline; relative weights of different SNVs and indels. **d.** BCM, IlluminaGA DNASeq, automated pipeline; count estimation using projection on the leading pattern.

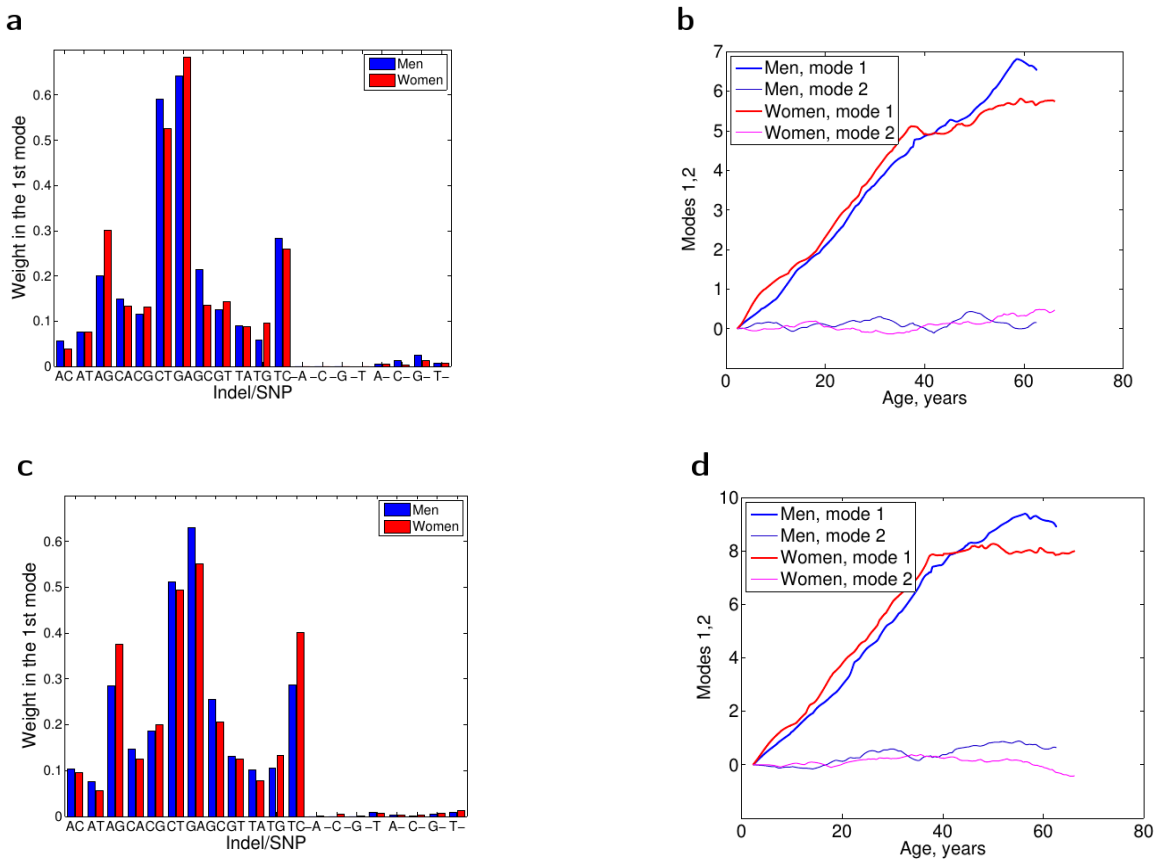

Supplementary Figure 63 | Modal structure of somatic mutation load in pheochromocytoma and paraganglioma (PCPG). **a.** BCGSC, IlluminaHiSeq DNASeq, automated pipeline; relative weights of different SNVs and indels. **b.** BCGSC, IlluminaHiSeq DNASeq, automated pipeline; count estimation using projection on the leading pattern. **c.** BCM, IlluminaGA DNASeq, automated pipeline; relative weights of different SNVs and indels. **d.** BCM, IlluminaGA DNASeq, automated pipeline; count estimation using projection on the leading pattern.

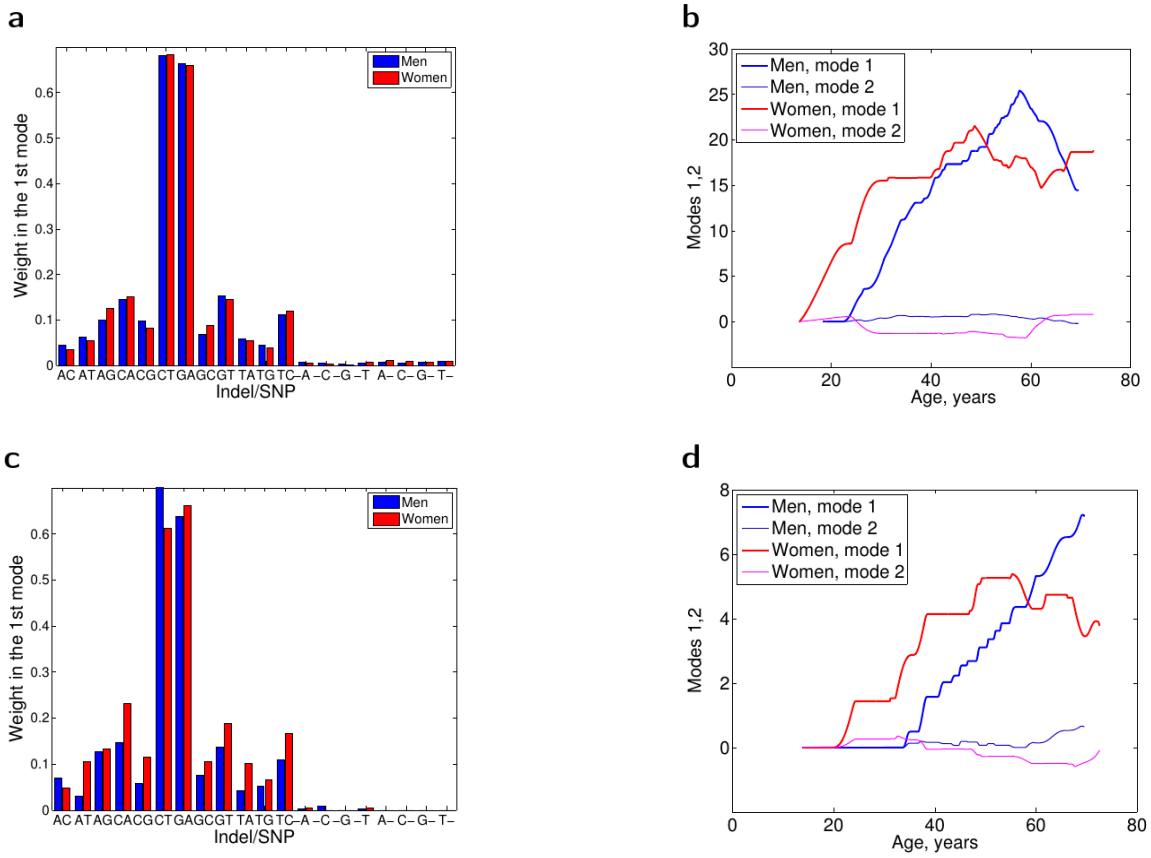

Supplementary Figure 64 | Modal structure of somatic mutation load in rectum adenocarcinoma (READ). **a.** BCM, IlluminaHiSeq DNASeq; relative weights of different SNVs and indels. **b.** BCM, IlluminaHiSeq DNASeq; count estimation using projection on the leading pattern. **c.** BCM, SOLiD DNASeq; relative weights of different SNVs and indels. **d.** BCM, SOLiD DNASeq; count estimation using projection on the leading pattern.

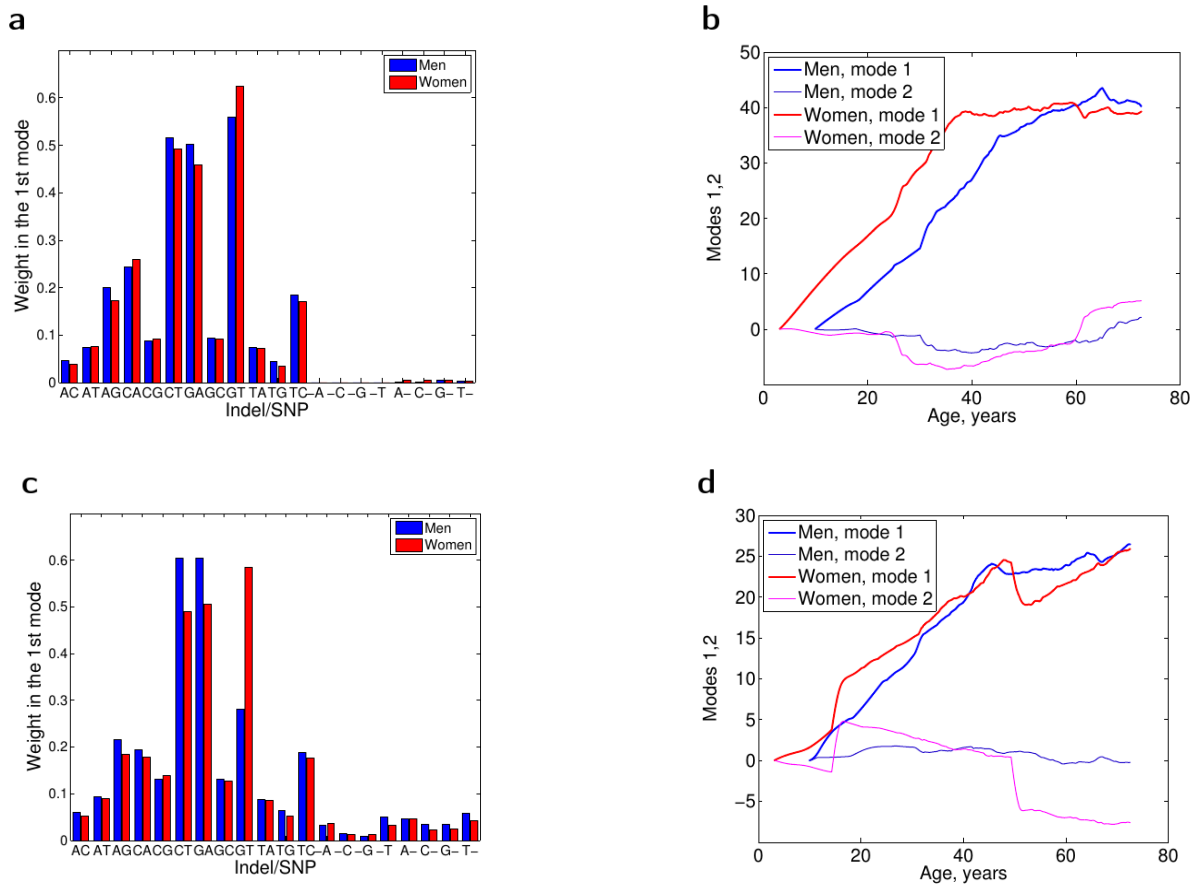

Supplementary Figure 65 | Modal structure of somatic mutation load in sarcoma (SARC). **a.** BCGSC, IlluminaHiSeq DNASeq, automated pipeline; relative weights of different SNVs and indels. **b.** BCGSC, IlluminaHiSeq DNASeq, automated pipeline; count estimation using projection on the leading pattern. **c.** BI, IlluminaGA DNASeq, automated pipeline; relative weights of different SNVs and indels. **d.** BI, IlluminaGA DNASeq, automated pipeline; count estimation using projection on the leading pattern.

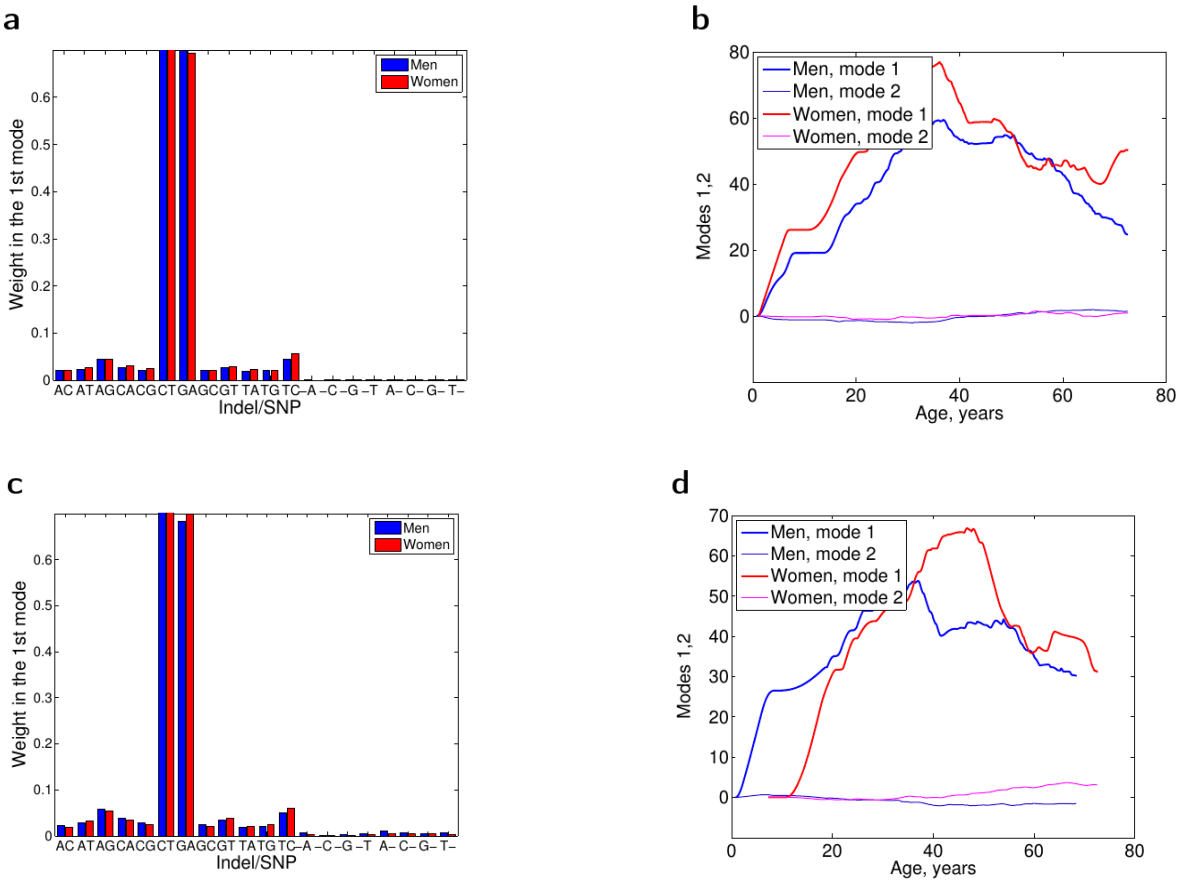

Supplementary Figure 66 | Modal structure of somatic mutation load in skin cutaneous melanoma (SKCM). **a.** BCM, IlluminaGA DNASeq, automated pipeline; relative weights of different SNVs and indels. **b.** BCM, IlluminaGA DNASeq, automated pipeline; count estimation using projection on the leading pattern. **c.** BI, IlluminaGA DNASeq, automated pipeline; relative weights of different SNVs and indels. **d.** BI, IlluminaGA DNASeq, automated pipeline; count estimation using projection on the leading pattern.

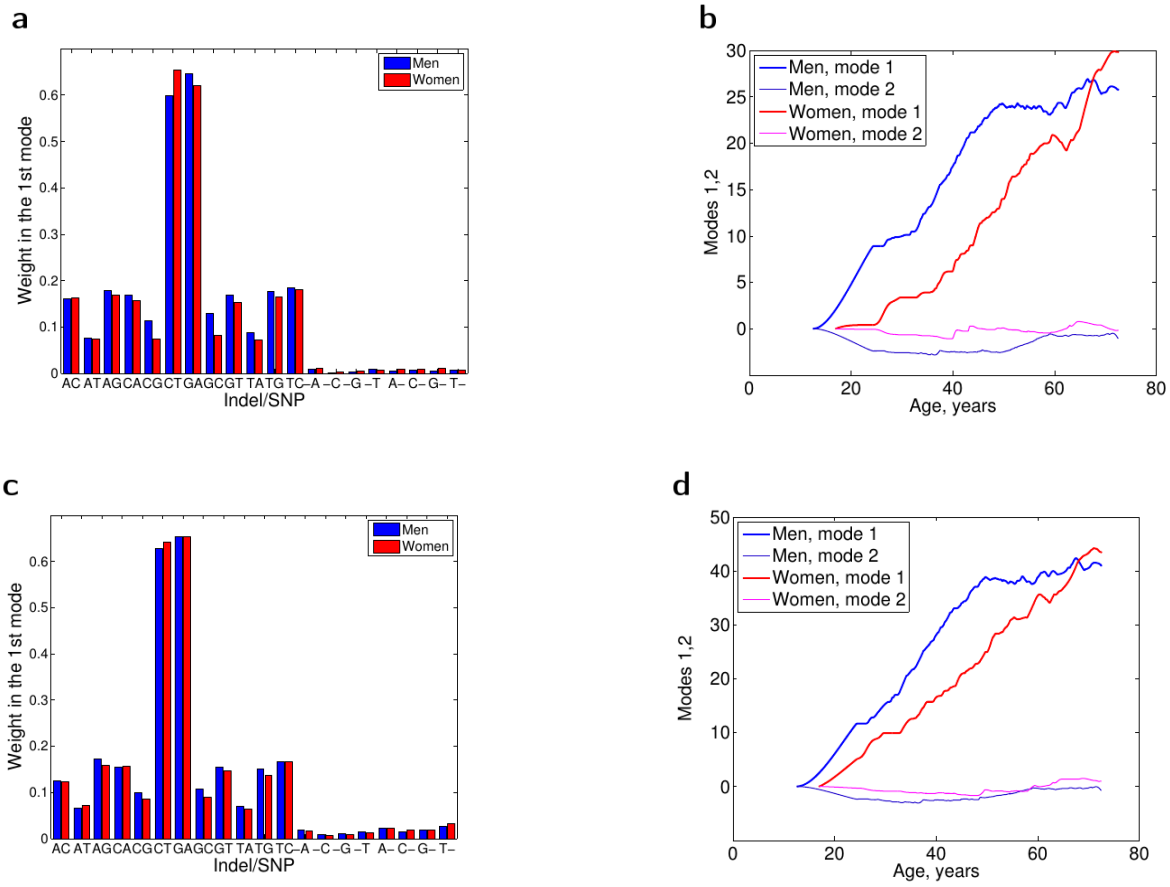

Supplementary Figure 67 | Modal structure of somatic mutation load in stomach adenocarcinoma (STAD). **a.** BCM, IlluminaGA DNASeq, automated pipeline; relative weights of different SNVs and indels. **b.** BCM, IlluminaGA DNASeq, automated pipeline; count estimation using projection on the leading pattern. **c.** BI, IlluminaGA DNASeq, automated pipeline; relative weights of different SNVs and indels. **d.** BI, IlluminaGA DNASeq, automated pipeline; count estimation using projection on the leading pattern.

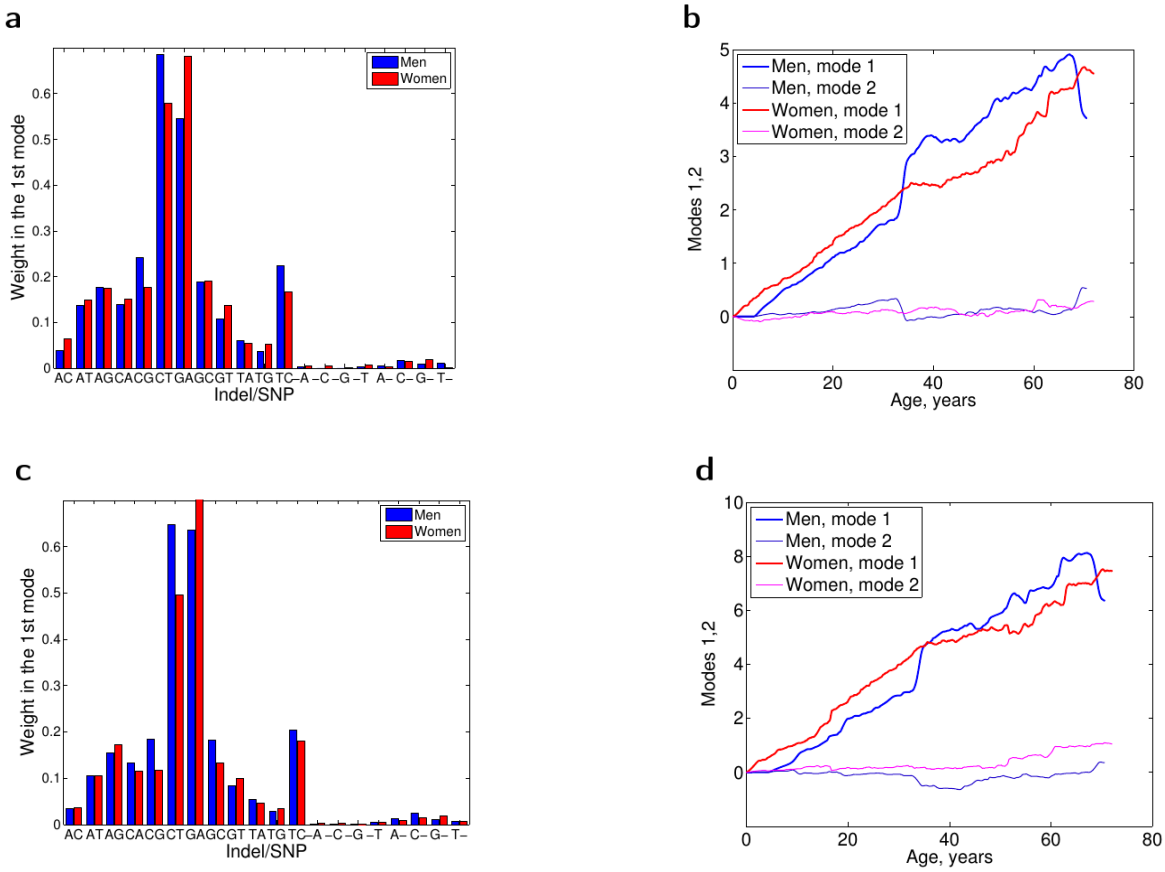

Supplementary Figure 68 | Modal structure of somatic mutation load in thyroid carcinoma (THCA). **a.** BCM, IlluminaGA DNASeq, automated pipeline; relative weights of different SNVs and indels. **b.** BCM, IlluminaGA DNASeq, automated pipeline; count estimation using projection on the leading pattern. **c.** BI, IlluminaGA DNASeq; relative weights of different SNVs and indels. **d.** BI, IlluminaGA DNASeq; count estimation using projection on the leading pattern.

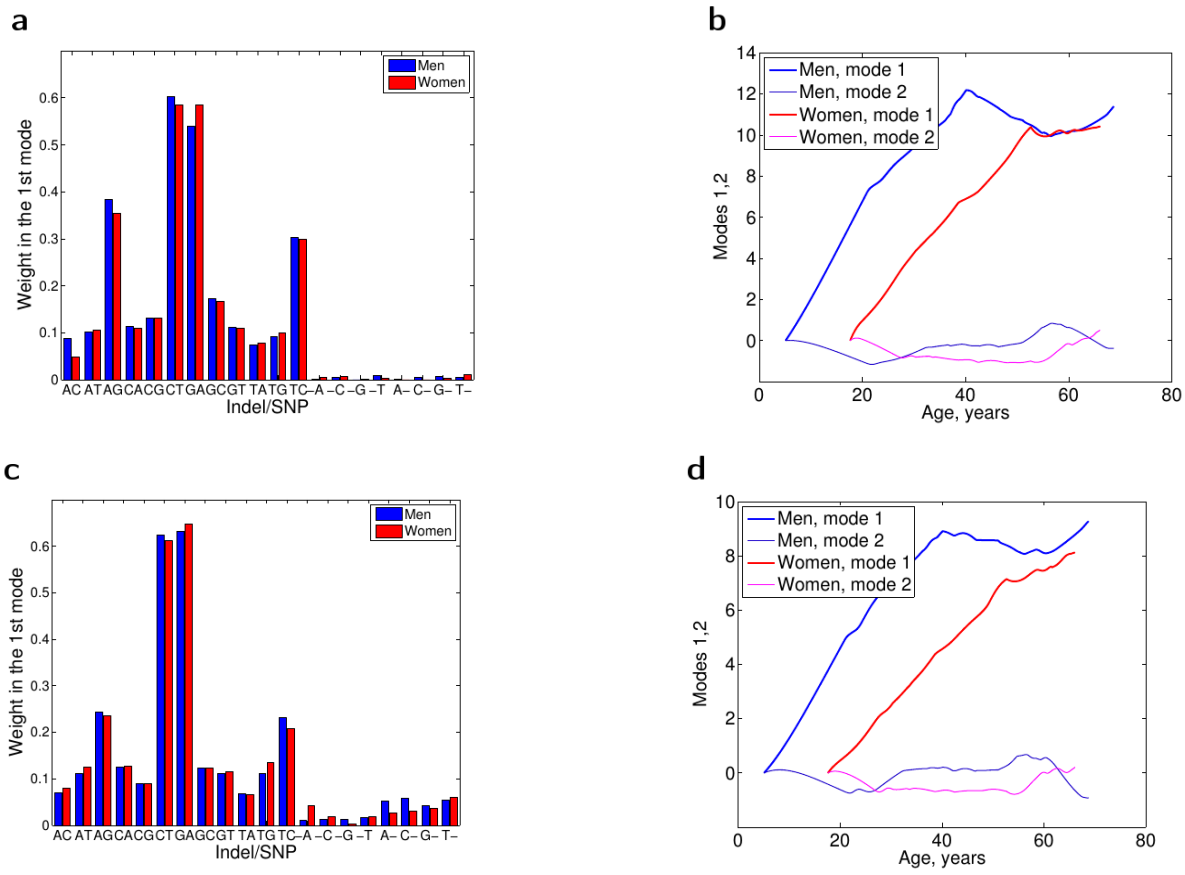

Supplementary Figure 69 | Modal structure of somatic mutation load in uveal melanoma (UVM). **a.** BCM, IlluminaGA DNASeq, automated pipeline; relative weights of different SNVs and indels. **b.** BCM, IlluminaGA DNASeq, automated pipeline; count estimation using projection on the leading pattern. **c.** BI, IlluminaGA DNASeq, automated pipeline; relative weights of different SNVs and indels. **d.** BI, IlluminaGA DNASeq, automated pipeline; count estimation using projection on the leading pattern.

Supplementary Table 1. Somatic mutation accumulation rates in different cancer types (women). Errors are s.d. determined by bootstrapping, see Methods.

Cancer	Datacenter, technology, pipeline	R_{full}, 1/year/exome	R_{silent}, 1/year/exome	α_{full}, 1/year	α_{silent}, 1/year
ACC	BCM,IlluminaGA,autom.	1.9429±0.0018	0.7747±0.0004	0.1407±0.0001	0.1457±0.0001
ACC	BCM,IlluminaGA,cur.	0.5744±0.0005	0.1536±0.0000	0.1301±0.0001	0.1404±0.0001
ACC	BCM,mixed,cur.	3.1138±0.0052	1.1939±0.0010	0.1407±0.0001	0.1466±0.0001
ACC	BI,IlluminaGA,cur.	1.2921±0.0009	0.2693±0.0000	0.1323±0.0001	0.1266±0.0001
BLCA	BI,IlluminaGA,	1.0181±0.0086	0.4339±0.0018	0.1238±0.0001	0.1680±0.0002
BLCA	BI,IlluminaGA,autom.	2.0762±0.0180	0.7617±0.0031	0.1228±0.0000	0.1594±0.0001
BLCA	BI,IlluminaGA,cur.	0.9689±0.0051	0.5299±0.0010	0.0860±0.0002	0.0731±0.0000
BRCA	WUSM,IlluminaGA	1.1525±0.0003	0.2262±0.0000	0.1341±0.0001	0.1462±0.0001
BRCA	WUSM,IlluminaGA,cur.	1.1922±0.0009	0.3339±0.0000	0.1532±0.0001	0.1587±0.0004
CESC	BCGSC,IlluminaHiSeq,autom.	2.7436±0.0063	1.3251±0.0038	0.1494±0.0001	0.1929±0.0002
CESC	BI,IlluminaGA	0.5505±0.0005	0.1718±0.0001	0.1635±0.0002	0.2284±0.0006
CESC	BI,IlluminaGA,autom.	0.5226±0.0004	0.1713±0.0001	0.1698±0.0003	0.2152±0.0005
CESC	UCSC,IlluminaGA,autom.	1.9090±0.0028	0.8186±0.0026	0.1802±0.0002	0.2266±0.0002
CESC	WUSM,IlluminaGA,cur.	2.4923±0.0031	0.8478±0.0024	0.1516±0.0002	0.2027±0.0002
CHOL	BCGSC,IlluminaHiSeq,autom.	0.2945±0.0006	0.0710±0.0000	0.0697±0.0000	0.0701±0.0000
CHOL	BCM,IlluminaGA,autom.	0.5789±0.0023	0.1622±0.0002	0.0808±0.0001	0.0997±0.0001
CHOL	BI,IlluminaGA,autom.	0.2873±0.0006	0.0562±0.0000	0.0744±0.0000	0.1004±0.0001
CHOL	UCSC,IlluminaGA,autom.	0.1604±0.0002	0.0529±0.0000	0.0758±0.0000	0.0944±0.0001
COAD	BCM,IlluminaGA	1.5759±0.0053	0.7315±0.0014	0.1408±0.0002	0.1621±0.0003
COAD	BCM,SOLiD	0.0637±0.0001	0.1003±0.0001	0.0266±0.0000	0.1225±0.0004
ESCA	BCGSC,IlluminaHiSeq,autom.	1.5824±0.0132	0.4244±0.0011	0.1139±0.0001	0.1281±0.0001
ESCA	BCM,IlluminaGA,autom.	2.0547±0.0210	0.5533±0.0017	0.1006±0.0000	0.1203±0.0001
ESCA	BI,IlluminaGA,autom.	1.4434±0.0117	0.4092±0.0011	0.1138±0.0001	0.1446±0.0001
ESCA	UCSC,IlluminaGA,autom.	1.3795±0.0118	0.3217±0.0006	0.1476±0.0001	0.1509±0.0001
GBM	BI,IlluminaGA	0.2446±0.0003	0.0554±0.0000	0.0952±0.0001	0.0951±0.0001
HNSC	BI,IlluminaGA	0.7703±0.0048	0.2471±0.0005	0.0561±0.0001	0.0705±0.0001
HNSC	BI,IlluminaGA,autom.	1.4736±0.0060	0.3949±0.0008	0.1621±0.0003	0.1633±0.0002
KICH	BCM,IlluminaGA	0.0677±0.0001	0.0126±0.0000	0.0926±0.0001	0.0972±0.0001
KICH	BCM,mixed,cur.	0.5056±0.0030	0.1297±0.0002	0.0849±0.0001	0.0848±0.0001
KICH	BI,IlluminaGA,	0.1801±0.0004	0.0343±0.0000	0.0798±0.0001	0.0904±0.0001
KIRC	BCM,mixed	0.7688±0.0035	0.1681±0.0002	0.1631±0.0000	0.1981±0.0001
KIRC	BI,IlluminaGA,autom.	0.7946±0.0006	0.4386±0.0008	0.1045±0.0001	0.1738±0.0001
KIRP	BCM,IlluminaGA,cur.	0.5469±0.0012	0.1296±0.0001	0.1139±0.0000	0.0956±0.0000
KIRP	BCM,Mixed,cur.	0.6573±0.0010	0.1569±0.0001	0.1125±0.0000	0.0972±0.0000

KIRP	BI,IlluminaGA	0.3288±0.0006	0.0677±0.0000	0.0594±0.0000	0.0447±0.0000
KIRP	BI,IlluminaGA,autom.	0.3697±0.0009	0.0653±0.0000	0.0629±0.0000	0.0448±0.0000
KIRP	BI,IlluminaGA,cur.	0.5798±0.0012	0.1171±0.0000	0.0837±0.0000	0.0640±0.0000
KIRP	UCSC,IlluminaGA,autom.	0.3606±0.0005	0.1557±0.0005	0.0984±0.0000	0.1215±0.0001
LAML	WUSM,IlluminaGA	0.2076±0.0001	0.0445±0.0000	0.1244±0.0001	0.1406±0.0003
LGG	BCM,IlluminaGA,autom.	0.3689±0.0002	0.1055±0.0000	0.1503±0.0000	0.1600±0.0001
LGG	BI,IlluminaGA	0.4227±0.0002	0.9229±0.0411	0.1314±0.0000	0.2523±0.0005
LGG	BI,IlluminaGA,autom.	1.0416±0.0012	1.0635±0.0468	0.1648±0.0001	0.2441±0.0003
LGG	BI,IlluminaGA,cur.	0.5981±0.0005	0.1339±0.0000	0.1417±0.0000	0.1507±0.0000
LIHC	BCGSC,IlluminaHiSeq,autom.	0.7157±0.0034	0.3764±0.0027	0.0790±0.0001	0.0885±0.0003
LIHC	BCM,IlluminaGA,autom.	0.3511±0.0013	0.0937±0.0001	0.1157±0.0003	0.1171±0.0003
LIHC	BCM,mixed,cur.	0.4919±0.0025	0.1212±0.0002	0.1158±0.0003	0.1137±0.0003
LIHC	BI,IlluminaGA,autom.	0.4816±0.0017	0.1624±0.0002	0.1031±0.0001	0.1122±0.0003
LIHC	UCSC,IlluminaGA,autom.	0.3653±0.0015	0.0851±0.0001	0.1107±0.0003	0.0972±0.0002
LUAD	BI,IlluminaGA	2.9307±0.0059	2.8546±0.0122	0.1305±0.0001	0.1317±0.0002
LUAD	BI,IlluminaGA,autom.	3.2698±0.0076	3.1238±0.0106	0.1371±0.0001	0.1392±0.0002
LUSC	BI,IlluminaGA	2.2059±0.0084	0.8414±0.0007	0.1243±0.0001	0.0983±0.0000
OV	BCM,SOLiD,cur.	0.1896±0.0000	0.0314±0.0000	0.1362±0.0001	0.1418±0.0001
OV	BI,IlluminaGA	0.2093±0.0000	0.0453±0.0000	0.1413±0.0003	0.1409±0.0002
OV	WUSM,IlluminaGA	0.5382±0.0032	0.1193±0.0002	0.2424±0.0002	0.2343±0.0002
PAAD	BCGSC,IlluminaHiSeq,autom.	1.2652±0.0012	2.9848±0.3132	0.1367±0.0001	0.2121±0.0024
PAAD	BCM,IlluminaGA,autom.	1.5968±0.0027	0.9587±0.0266	0.1299±0.0001	0.1805±0.0014
PAAD	BI,IlluminaGA	0.6053±0.0009	1.1815±0.0455	0.0833±0.0001	0.1629±0.0003
PAAD	BI,IlluminaGA,autom.	3.8809±0.0125	1.9321±0.0535	0.1361±0.0001	0.1652±0.0001
PAAD	UCSC,IlluminaGA,autom.	0.6379±0.0016	0.3144±0.0104	0.1264±0.0003	0.1583±0.0005
PCPG	BCGSC,IlluminaHiSeq,autom.	0.1433±0.0000	0.0368±0.0000	0.1059±0.0000	0.0793±0.0000
PCPG	BCM,IlluminaGA,autom.	0.2730±0.0001	0.0434±0.0000	0.1180±0.0001	0.0959±0.0000
PCPG	BI,IlluminaGA,autom.	0.2672±0.0001	0.0480±0.0000	0.1081±0.0001	0.0841±0.0000
PCPG	UCSC,IlluminaGA,autom.	0.1525±0.0001	0.0460±0.0000	0.1063±0.0000	0.0846±0.0000
READ	BCM,IlluminaGA	0.4438±0.0013	0.1396±0.0002	0.1082±0.0001	0.1222±0.0001
READ	BCM,SOLiD	0.3904±0.0008	0.0975±0.0001	0.1350±0.0001	0.1235±0.0001
SARC	BCGSC,IlluminaHiSeq,autom.	0.8523±0.0019	0.7174±0.0038	0.1208±0.0000	0.2012±0.0002
SARC	BI,IlluminaGA,autom.	0.8240±0.0034	0.1366±0.0001	0.1546±0.0001	0.1546±0.0001
SARC	UCSC,IlluminaGA,autom.	0.3827±0.0008	0.2152±0.0003	0.1527±0.0000	0.1850±0.0002
SKCM	BCM,IlluminaGA,autom.	2.1306±0.0247	2.6886±0.0809	0.1006±0.0000	0.1149±0.0001
SKCM	BI,IlluminaGA	2.9425±0.0143	3.9496±0.0519	0.1422±0.0003	0.0790±0.0001
SKCM	BI,IlluminaGA,autom.	2.9309±0.0199	4.2844±0.0604	0.1410±0.0004	0.0806±0.0001
STAD	BCGSC,IlluminaHiSeq,autom.	0.3740±0.0015	0.0951±0.0002	0.1078±0.0001	0.0991±0.0001
STAD	BCM,IlluminaGA,autom.	0.4049±0.0009	0.4030±0.0061	0.1768±0.0003	0.2684±0.0004
STAD	BI,IlluminaGA	1.3536±0.0028	1.8059±0.0097	0.1031±0.0000	0.2120±0.0003

STAD	BI,IlluminaGA,autom.	1.1559±0.0046	0.6909±0.0147	0.1962±0.0003	0.2686±0.0003
STAD	BI,IlluminaGA,cur.	0.5146±0.0015	0.5878±0.0133	0.1643±0.0002	0.2577±0.0004
THCA	BCM,IlluminaGA,autom.	0.1994±0.0000	0.0529±0.0000	0.1706±0.0005	0.1503±0.0004
THCA	BI,IlluminaGA	0.3211±0.0001	0.0751±0.0000	0.1525±0.0003	0.1436±0.0001
UCEC	BI,IlluminaGA	1.0686±0.0008	0.4332±0.0008	0.1576±0.0003	0.1333±0.0002
UCEC	WUSM,IlluminaGA	0.6860±0.0003	2.3757±0.0314	0.1573±0.0002	0.0313±0.0000
UCS	BCM,IlluminaGA,autom.	1.1407±0.0029	0.3411±0.0003	0.1425±0.0001	0.1578±0.0001
UCS	BI,IlluminaGA,autom.	1.7946±0.0066	0.3893±0.0005	0.1420±0.0001	0.1684±0.0001
UCS	BI,IlluminaGA,cur.	1.6217±0.0049	0.4064±0.0006	0.1404±0.0001	0.1561±0.0001
UVM	BCGSC,IlluminaHiSeq,autom.	0.2281±0.0002	0.3186±0.0022	0.1002±0.0000	0.2006±0.0011
UVM	BCM,IlluminaGA,autom.	0.3063±0.0004	0.3470±0.0017	0.0801±0.0000	0.1281±0.0004
UVM	BI,IlluminaGA,autom.	0.2329±0.0002	0.3376±0.0026	0.0965±0.0000	0.2171±0.0014
UVM	UCSC,IlluminaGA,autom.	0.1496±0.0001	0.2160±0.0010	0.1083±0.0001	0.1827±0.0009

Supplementary Table 2. Somatic mutation accumulation rates in different cancer types (men). Errors are s.d., determined by bootstrapping, see Methods.

Cancer	Datacenter, technology, pipeline	R_{full}, 1/year/exome	R_{silent}, 1/year/exome	α_{full}, 1/year	α_{silent}, 1/year
ACC	BCM,IlluminaGA,autom.	0.0945±0.0002	0.2139±0.0013	0.0263±0.0000	0.0763±0.0001
ACC	BCM,IlluminaGA,cur.	0.0871±0.0001	0.1668±0.0009	0.0652±0.0001	0.1535±0.0003
ACC	BCM,mixed,cur.	0.1717±0.0006	0.3671±0.0036	0.0315±0.0000	0.0898±0.0001
ACC	BI,IlluminaGA,cur.	0.0617±0.0001	0.2149±0.0017	0.0363±0.0000	0.1689±0.0006
BLCA	BI,IlluminaGA	0.4243±0.0011	0.2031±0.0001	0.1182±0.0001	0.0761±0.0001
BLCA	BI,IlluminaGA,autom.	1.6079±0.0135	0.8930±0.0069	0.1619±0.0000	0.2175±0.0001
BLCA	BI,IlluminaGA,cur.	0.6858±0.0073	0.5933±0.0067	0.1574±0.0002	0.2329±0.0005
BRCA	WUSM,IlluminaGA	0.1861±0.0007	0.0385±0.0000	0.0492±0.0000	0.0465±0.0000
BRCA	WUSM,IlluminaGA,cur.	0.2011±0.0004	0.0487±0.0000	0.0561±0.0000	0.0570±0.0000
CHOL	BCGSC,IlluminaHiSeq,autom.	1.0173±0.0028	0.1947±0.0001	0.1138±0.0000	0.1076±0.0001
CHOL	BCM,IlluminaGA,autom.	1.8091±0.0070	0.3916±0.0003	0.1139±0.0001	0.1164±0.0001
CHOL	BI,IlluminaGA,autom.	1.6668±0.0082	0.2457±0.0001	0.1050±0.0000	0.0938±0.0000
CHOL	UCSC,IlluminaGA,autom.	0.9276±0.0040	0.1863±0.0001	0.1211±0.0000	0.1185±0.0000
COAD	BCM,IlluminaGA	0.8474±0.0021	2.4542±0.0331	0.1071±0.0001	0.0849±0.0001
COAD	BCM,SOLiD	0.1058±0.0001	0.0524±0.0001	0.1164±0.0002	0.1395±0.0002
ESCA	BCGSC,IlluminaHiSeq,autom.	1.6260±0.0554	0.4185±0.0041	0.1171±0.0001	0.1293±0.0002
ESCA	BCM,IlluminaGA,autom.	1.9787±0.0699	0.5349±0.0060	0.1312±0.0001	0.1412±0.0002
ESCA	BI,IlluminaGA,autom.	1.5338±0.0504	0.3719±0.0037	0.1194±0.0001	0.1368±0.0002
ESCA	UCSC,IlluminaGA,autom.	1.2706±0.0369	0.3056±0.0023	0.1201±0.0001	0.1188±0.0002
GBM	BI,IlluminaGA	0.3712±0.0003	0.0743±0.0000	0.1292±0.0002	0.1203±0.0001
HNSC	BI,IlluminaGA	0.4938±0.0018	0.1337±0.0004	0.0863±0.0000	0.1034±0.0001
HNSC	BI,IlluminaGA,autom.	0.7247±0.0013	0.1910±0.0003	0.1189±0.0001	0.1156±0.0000
KICH	BCM,IlluminaGA	0.1618±0.0001	0.0407±0.0000	0.1079±0.0000	0.1117±0.0000
KICH	BCM,Mixed,cur.	1.0396±0.0044	0.2616±0.0004	0.1128±0.0000	0.1200±0.0000
KICH	BI,IlluminaGA,	0.4409±0.0008	0.0888±0.0000	0.1126±0.0000	0.1214±0.0000
KIRC	BCM,mixed	0.7405±0.0030	0.1780±0.0002	0.2325±0.0003	0.2628±0.0005
KIRC	BI,IlluminaGA,autom.	0.7046±0.0005	0.2813±0.0005	0.1062±0.0001	0.1207±0.0005
KIRP	BCM,IlluminaGA,cur.	0.8734±0.0064	0.2454±0.0005	0.1763±0.0002	0.1673±0.0001
KIRP	BCM,mixed,cur.	1.0116±0.0107	0.2501±0.0006	0.1733±0.0001	0.1624±0.0001
KIRP	BI,IlluminaGA	0.6483±0.0040	0.1405±0.0002	0.1574±0.0001	0.1376±0.0001
KIRP	BI,IlluminaGA,autom.	0.7444±0.0055	0.1590±0.0003	0.1753±0.0002	0.1510±0.0001
KIRP	BI,IlluminaGA,cur.	1.1436±0.0132	0.2687±0.0008	0.1984±0.0002	0.1833±0.0002
KIRP	UCSC,IlluminaGA,autom.	1.8955±0.0050	1.0576±0.0063	0.1439±0.0003	0.1149±0.0002
LAML	WUSM,IlluminaGA	0.1726±0.0001	0.0379±0.0000	0.1586±0.0004	0.1708±0.0005
LGG	BCM,IlluminaGA,autom.	0.3318±0.0003	0.0672±0.0000	0.1600±0.0001	0.1609±0.0000
LGG	BI,IlluminaGA	0.4224±0.0005	0.0742±0.0000	0.1425±0.0001	0.1754±0.0001

LGG	BI,IlluminaGA,autom.	0.9809±0.0019	0.1678±0.0001	0.1904±0.0001	0.1999±0.0002
LGG	BI,IlluminaGA,cur.	0.5404±0.0005	0.0810±0.0000	0.1603±0.0001	0.1726±0.0000
LIHC	BCGSC,IlluminaHiSeq,autom.	1.3393±0.0114	0.7262±0.0072	0.1735±0.0002	0.0389±0.0001
LIHC	BCM,IlluminaGA,autom.	0.4983±0.0005	0.6117±0.0060	0.0699±0.0000	0.0731±0.0005
LIHC	BCM,mixed,cur.	1.1337±0.0059	0.4553±0.0072	0.0927±0.0000	0.0540±0.0004
LIHC	BI,IlluminaGA,autom.	1.0842±0.0037	0.4638±0.0071	0.1543±0.0003	0.0539±0.0004
LIHC	UCSC,IlluminaGA,autom.	0.7949±0.0010	0.3041±0.0059	0.0691±0.0000	0.0432±0.0003
LUAD	BI,IlluminaGA	2.7142±0.0098	4.2332±0.0084	0.1412±0.0005	0.1395±0.0001
LUAD	BI,IlluminaGA,autom.	3.2160±0.0065	4.1589±0.0110	0.1492±0.0004	0.1385±0.0001
LUSC	BI,IlluminaGA	1.3383±0.0026	0.9408±0.0005	0.0748±0.0001	0.0477±0.0000
PAAD	BCGSC,IlluminaHiSeq,autom.	0.4994±0.0025	0.1488±0.0004	0.0997±0.0000	0.1115±0.0001
PAAD	BCM,IlluminaGA,autom.	0.5629±0.0014	0.0874±0.0000	0.0808±0.0000	0.0891±0.0000
PAAD	BI,IlluminaGA	0.6100±0.0038	0.0800±0.0001	0.0996±0.0001	0.0843±0.0001
PAAD	BI,IlluminaGA,autom.	1.7058±0.0074	0.2139±0.0001	0.1023±0.0001	0.1127±0.0001
PAAD	UCSC,IlluminaGA,autom.	0.1500±0.0002	0.0392±0.0000	0.0695±0.0000	0.0606±0.0000
PCPG	BCGSC,IlluminaHiSeq,autom.	0.2388±0.0001	0.0439±0.0000	0.1159±0.0000	0.0861±0.0000
PCPG	BCM,IlluminaGA,autom.	0.4127±0.0002	0.0615±0.0000	0.1245±0.0000	0.1055±0.0000
PCPG	BI,IlluminaGA,autom.	0.4357±0.0002	0.0696±0.0000	0.1252±0.0000	0.1357±0.0001
PCPG	UCSC,IlluminaGA,autom.	0.2286±0.0001	0.0541±0.0000	0.1220±0.0000	0.1196±0.0001
PRAD	BCM,IlluminaGA,autom.	0.6015±0.0003	0.1974±0.0000	0.1246±0.0002	0.1172±0.0001
PRAD	BI,IlluminaGA,autom.	1.2047±0.0001	0.2725±0.0000	0.1342±0.0002	0.1552±0.0003
PRAD	BI,IlluminaGA,cur.	1.1487±0.0001	0.2611±0.0000	0.1316±0.0002	0.1528±0.0003
READ	BCM,IlluminaGA	1.8285±0.0023	1.2048±0.0212	0.1197±0.0001	0.0263±0.0000
READ	BCM,SOLiD	0.4171±0.0003	N/A	0.1231±0.0001	N/A
SARC	BCGSC,IlluminaHiSeq,autom.	0.9468±0.0029	0.2607±0.0003	0.1092±0.0000	0.0943±0.0002
SARC	BI,IlluminaGA,autom.	0.9357±0.0016	0.1491±0.0001	0.1018±0.0002	0.1023±0.0002
SARC	UCSC,IlluminaGA,autom.	0.4724±0.0008	0.1179±0.0000	0.1043±0.0003	0.1168±0.0002
SKCM	BCM,IlluminaGA,autom.	1.7010±0.0162	2.6219±0.0210	0.0838±0.0000	0.1249±0.0001
SKCM	BI,IlluminaGA	1.7919±0.0275	3.1573±0.0251	0.0773±0.0000	0.1248±0.0001
SKCM	BI,IlluminaGA,autom.	1.0395±0.0138	3.2819±0.0229	0.0533±0.0001	0.1248±0.0001
STAD	BCGSC,IlluminaHiSeq,autom.	0.3589±0.0011	0.0857±0.0001	0.0529±0.0001	0.0605±0.0001
STAD	BCM,IlluminaGA,autom.	1.4883±0.0086	1.0617±0.0043	0.1370±0.0000	0.1878±0.0005
STAD	BI,IlluminaGA	2.0189±0.0093	1.0874±0.0055	0.1357±0.0001	0.1866±0.0006
STAD	BI,IlluminaGA,autom.	3.1120±0.0094	1.4803±0.0064	0.1528±0.0001	0.2065±0.0006
STAD	BI,IlluminaGA,cur.	1.8112±0.0111	1.2758±0.0063	0.1367±0.0000	0.2036±0.0006
TGCT	BCGSC,IlluminaHiSeq_autom.	0.7363±0.0005	1.6580±0.0319	0.1962±0.0003	0.3707±0.0006
TGCT	BCM,IlluminaGA,autom.	0.6170±0.0003	0.1448±0.0000	0.1941±0.0003	0.2378±0.0006
TGCT	BI,IlluminaGA,autom.	1.2249±0.0013	0.2745±0.0000	0.1645±0.0001	0.1473±0.0002
TGCT	UCSC,IlluminaGA,autom.	0.5448±0.0007	0.1850±0.0001	0.2167±0.0003	0.2294±0.0002
THCA	BCM,IlluminaGA,autom.	0.1573±0.0000	0.0413±0.0000	0.1217±0.0001	0.1093±0.0000

THCA	BI,IlluminaGA	0.2861±0.0001	0.0509±0.0000	0.1597±0.0002	N/A
UVM	BCGSC,IlluminaHiSeq_autom.	0.0847±0.0004	0.0135±0.0000	0.0642±0.0002	0.0589±0.0002
UVM	BCM,IlluminaGA,autom.	0.1240±0.0007	0.0405±0.0001	0.0599±0.0002	0.0578±0.0001
UVM	BI,IlluminaGA,autom.	0.1011±0.0005	0.0113±0.0000	0.0650±0.0002	0.0642±0.0002
UVM	UCSC,IlluminaGA,autom.	0.0650±0.0002	0.0146±0.0000	0.0749±0.0002	0.1221±0.0006

Supplementary Table 3. Median chronological ages of screened individuals with samples present in TCGA vs. median chronological ages of cancer incidence for women.

Cancer type	Median age of cancer incidence	Median age of screened individuals (TCGA)
BLCA	52.5	73
BRCA	46.4	59
CESC	32	46
COAD	52.5	68
HNSC	45	64
LIHC	45	63
OV	45	59
PAAD	50	64
READ	54.7	66.5
SKCM	39.4	58
STAD	52.5	69
THCA	29.3	46
UCEC	44.8	64
UCS	44.8	69
UVM	45	60

Supplementary Table 4. Median chronological ages of screened individuals with samples present in TCGA vs. median chronological ages of cancer incidence for men.

Cancer type	Median age of cancer incidence	Median age of screened individuals (TCGA)
BLCA	45	68
BRCA	46	61
COAD	52.5	69
HNSC	41	60
LIHC	45	60.5
PAAD	52.5	67
PRAD	45	61
READ	51.3	65
SKCM	45	57
STAD	55	66
TGCT	13.4	31
THCA	36.4	50.5
UVM	42.9	64